nature reviews physics

https://doi.org/10.1038/s42254-026-00925-w

Review article

Check for updates

Physics of sphere packings

Salvatore Torquato [1,2,3,4]

Abstract

The fundamental study of ordered and disordered sphere packings provides deep physical insights about the structural and bulk physical properties of equilibrium and nonequilibrium phases of matter, and continues to offer tantalizing mathematical challenges. During the past three decades, there has been a flurry of developments on sphere packing problems across spatial dimensions in physics and mathematics. The purpose of this Review is to survey this progress in the case of frictionless identical (monodisperse) hard spheres, while placing it in the context of earlier classic investigations.

Sections

Introduction

Sphere packings in low dimensions

Sphere packings in high dimensions

Outlook

[1]Department of Chemistry, Princeton University, Princeton, NJ, USA. [2]Department of Physics, Princeton University, Princeton, NJ, USA. [3]Princeton Materials Institute, Princeton University, Princeton, NJ, USA. [4]Program in Applied and Computational Mathematics, Princeton University, Princeton, NJ, USA. e-mail: torquato@princeton.edu

Key points

- Sphere packings across space dimensions are shown to provide basic insights into the structure and bulk properties of condensed phases of matter, such as liquids, glasses and crystals, and phase transitions between them.
- Equilibrium and nonequilibrium packings are considered with varying degrees of order and disorder, and that may or may not be jammed.
- Packings in space dimensions greater than three, which are of great interest to physicists and mathematicians, are discussed.
- Emphasis is placed on rigorous methods and, in the case of dense disordered or ordered packings, on the 'geometric-structure' approach, which analyses single-packing configurations (disordered or not), without regard to their frequency of occurrence.
- The formulation of sensitive order metrics to quantitatively characterize many-body systems is an outstanding problem in statistical and condensed-matter physics.

Introduction

Particle packings — large collections of nonoverlapping particles (also known as hard particles) of general shape in a volume in space — are ubiquitous in nature and synthetic contexts. Their study has attracted the attention of luminaries of science, including but not limited to Johannes Kepler[1], Hermann Minkowski[2], John Desmond Bernal[3] and Claude Shannon[4], and continues to be a subject of intense research across contexts in the physical, mathematical and biological sciences[4–24]. The quantitative characterization of particle packings provides basic insights into the structure and bulk properties of condensed phases of matter, such as liquids, glasses and crystals, and phase transitions between them[9,12,18], and, in high spatial dimensions, their quantitative characterization has relevance in the study of certain aspects of quantum gravity[21,23]. Because particle packings accurately capture salient exclusion-volume effects inherent in dense many-particle systems, they often provide good structural models of heterogeneous media, including composites, suspensions, granular media, powders, colloids and geological media[6,7,11–13,19,24]. Biology is replete with examples of particle packings, including phyllotaxis[7], macromolecular crowding within cells[10], DNA packaging[11], photoreceptor mosaics[19] and cell packings in developing tissue[22]. The investigation of the mathematical properties (such as symmetries and spatial arrangements) of the densest sphere packings in various spaces and dimensions has been of great interest in discrete geometry[1,5,8], number theory[8,14], cryptography[8] and coding theory[4,8].

This Review covers selected past and recent developments related to the simplest yet classic packing model: nonoverlapping, identical (congruent), frictionless spheres in d-dimensional Euclidean space $\mathbb{R}^d$ in the absence of any external field (such as gravity). I examine, across spatial dimensions, equilibrium and nonequilibrium sphere packings with varying degrees of order and disorder, and that may or may not be jammed. Emphasis is placed on rigorous methods to the extent possible and, in the case of dense disordered or ordered packings, on the geometric-structure approach[17,20], which requires the quantification of sensitive order metrics — an outstanding problem in statistical and condensed-matter physics.

Other reviews on disordered packings of identical spheres include refs. 16,25–27; these do not specifically focus on the geometric-structure approach to analyse such packings or the densest packings in high dimensions. Sphere packings involving size distributions (polydispersity), which give rise to a wide range of ordered and disordered phases owing to the infinite-dimensional parameter space (all sphere size ratios and relative concentrations), fall outside the scope of this Review. For comprehensive surveys on these topics, the reader is referred to refs. 17,20 and references therein. Similarly, packings in curved spaces — such as hyperbolic or compact spaces (the surface of a d-dimensional sphere, for example) — and packings of nonspherical particles (such as ellipsoids, superballs and polyhedra) are also discussed in refs. 17,20.

Sphere packings in low dimensions

A basic characteristic of a sphere packing is the packing fraction ϕ, which is the fraction of space $\mathbb{R}^d$ covered by the spheres. For identical spheres of diameter D at number density ρ in $\mathbb{R}^d$, $\phi = \rho v_1(D/2)$, where $v_1(R) = \pi^{d/2}R^d/\Gamma(1+d/2)$ is the volume of a d-dimensional sphere of radius R. The focus of this section is primarily on various disordered sphere packings, as well as the densest sphere packings in the first three space dimensions. A disordered packing is one without long-range order (indicated by the absence of Bragg peaks, for example) and whose n-particle correlation function g_n approaches unity as the particles become well-separated from one another[12]. Roughly speaking, a periodic packing is characterized by long-range translational and orientational order (an infinite set of Bragg peaks reflecting crystallographic symmetries, for example). The reader is referred to refs. 17,20 for precise mathematical definitions concerning basic aspects of packings.

Equilibrium and metastable packings

The classical statistical mechanics of hard spheres in equilibrium (Gibbs ensembles) has attracted great attention over the years[18,28–30], dating back at least to Ludwig Boltzmann[31]. Such systems for relatively low dimensions greater than one represent the simplest models that exhibit a phase transition from disordered to ordered states at sufficiently high packing fractions. The phase behaviour of hard spheres offers valuable insights into the nature of liquids, crystals, metastable states and the phase transitions that arise in actual molecular and colloidal systems. In $\mathbb{R}^d$, the pressure p of a stable thermodynamic hard-sphere phase at packing fraction ϕ and temperature T is directly related to the contact value of the pair correlation function[12,18], $g_2(D^+)$, namely:

$$\frac{p}{\rho k_B T} = 1 + 2^{d-1}\phi g_2(D^+) = -\phi\frac{\mathrm{d}s(\phi)}{\mathrm{d}\phi}. \quad (1)$$

Here, $s(\phi)$ is the entropy per particle at packing fraction ϕ, which can be obtained by integration of equation (1).

The 3D phase behaviour in the ϕ–p plane is schematically shown in Fig. 1. Starting at low densities, an infinitesimally slow compression of the system at constant temperature traces out a thermodynamically stable liquid branch for packing fractions up to the 'freezing' point ($\phi_F \approx 0.49$)[32]. The Percus–Yevick closure of the Ornstein–Zernike integral equation yields relatively accurate approximations of the pair correlation functions along the stable liquid branch[18]. Slowly increasing ϕ beyond the freezing point putatively results in an entropically driven first-order phase transition[28,33] to a crystal branch that starts at the melting point ($\phi_M \approx 0.55$)[32]. Slow compression along the crystalline branch ultimately leads to one of the optimal (maximally dense) sphere

packings with a packing fraction $\phi = \pi/\sqrt{18} = 0.74048\ldots$. Each of these configurations is a 'strictly' jammed state, in which every particle is in contact with 12 neighbours (see the 'Jamming categories' subsection). This equilibrium state has an infinite pressure and is putatively entropically favoured by the face-centred-cubic (fcc) packing[34]. A careful Monte Carlo study of the 2D equilibrium hard-disk model reveals that freezing (where $\phi_F \approx 0.69$)[32] proceeds in two steps: a first-order liquid–hexatic phase transition and continuous hexatic–solid phase transition[35], wherein the melting point is $\phi_M \approx 0.72$. Note that arbitrarily large 'holes' can exist along stable crystal phases below jamming points, even if such events are rare. Such large-hole statistics along 2D and 3D crystal branches are discussed in ref. 36.

When a 3D liquid of identical (monodisperse) hard spheres is compressed above the freezing point rapidly enough to suppress local ordering, crystal nucleation can be avoided over certain timescales[37]. As the density increases along this metastable extension of the liquid, the dynamics becomes progressively slower, and eventually (at and above some sufficiently high density) the free volume decreases to such an extent that the particles become 'caged' on large timescales. At such high densities of long-lasting metastable states, it is meaningful to decompose the total entropy S into a sum of a vibrational contribution S_v (owing to the entropy associated with the rattling of particles around the metastable states) and a configurational contribution S_c (number of accessible metastable liquid states at some sufficiently high density). The latter is given by the logarithm of the number of states, which is a decreasing function of ϕ. In analogy with the picture of an ideal glass transition in supercooled liquids[38], an ideal glass transition might be expected to occur at the so-called Kauzmann packing fraction ϕ_K (below any jammed density) when the configurational entropy S_c vanishes. Numerically, ϕ_K is estimated by extrapolating data for S_c at lower densities to zero[39–41]. The replica method has been applied to investigate the possibility of an ideal glass transition of a liquid of identical hard spheres[42]. Specifically, approximations of the configurational entropy in the liquid phase yield a ϕ_K that lies in the range 0.58–0.62, the uncertainties of which depend on the various approximations used for the equation of state. It is posited that this ideal glass jams at the so-called glass close packing, whose packing fraction ϕ_{GCP} is estimated to be 0.6836 (ref. 16), which is higher than the random close packing or maximally random jammed values, described below.

Whether there is any observable long-lived glass in 3D monodisperse hard-sphere systems above the freezing density but below jamming-point densities is still an open question. There is strong numerical evidence that metastable monodisperse hard-sphere systems always crystallize on relatively short timescales[37,43], that is, crystallization pre-empts the glass transition for monodisperse hard spheres. The absence of a glass transition has also been verified in experiments with hard-sphere colloidal systems in microgravity[44]. In the case of 2D hard-disk systems, the tendency of disordered states to crystallize below jamming (under conventional compression protocols) is even greater than in 3D, owing to the favourable formation of locally dense triangular arrangements of particles that are consistent with the globally dense arrangement. Meanwhile, a sufficiently high degree of polydispersity in size tends to supress crystallization and promotes glass formation over large timescales[45–49].

A sufficiently rapid compression process can lead to a range of amorphous, metastable extensions of the liquid branch that terminate at their respective maximum-density jammed states (as discussed and defined rigorously below)[12,37,50]. These jammed states can be interpreted as prototypical glasses. The most rapid compression

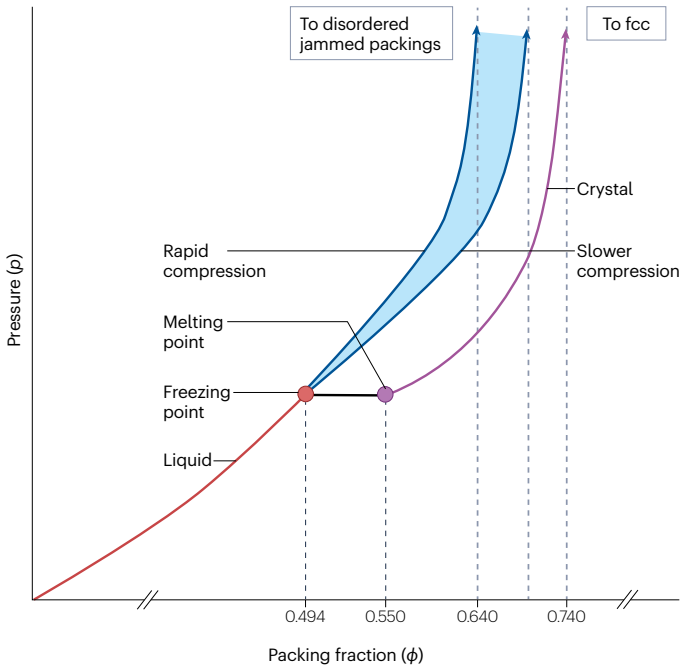


Fig. 1 | The isothermal phase behaviour of the 3D hard-sphere model in the pressure-packing fraction plane. An infinitesimal compression rate of the liquid traces out the thermodynamic equilibrium path (red curve), including a discontinuity in the first derivative resulting from the first-order freezing transition (black line) to a thermodynamically stable crystal branch (purple curve). Three different isothermal densification paths by which a hard-sphere liquid may jam are shown, two of which are disordered nonequilibrium states (end points of blue curves) and one of which is the maximally dense stable crystal state (end point of the purple curve). Figure adapted with permission from ref. 17, APS.

ending in a mechanically stable packing is presumably the maximally random jammed (MRJ) state[51] with $\phi \approx 0.64$. It is plausible that the highest-density jammed disordered state associated with the least rapid compression corresponds to glass close packing[16]. Accurate approximate formulas for the pressure along such metastable extensions up to the jamming points have been obtained[12,52].

Unjammed nonequilibrium packings

The statistical ensemble of the idealized hard-sphere model is not uniquely specified by the impenetrability constraint. The system can be in thermal equilibrium, as discussed above, or derived from one of an infinite number of nonequilibrium ensembles[12], two important examples of which are discussed in this section: random sequential addition (RSA) and ghost random sequential addition. Both of these packings are 'unjammed' because spheres cannot form any interparticle contacts. Nonetheless, both models teach us basic lessons about disordered and ordered packings, including the fact that they yield lower bounds on the maximal density among all packings in a given dimension, because the densest packing must be jammed.

Random sequential addition. The RSA packing procedure is a well-known time-dependent process that generates disordered sphere packings in $\mathbb{R}^d$ (see refs. 53–61). In the first three space dimensions, it has been used to model a variety of physical and biological processes and systems, including particles in cell membranes[55], protein

adsorption[56], settlement of territories by animals[62], polymer oxidation[63] and ion implantation in semiconductors[64]. An RSA packing of spheres is obtained by placing nonoverlapping spheres randomly, irreversibly and sequentially into a large volume in $\mathbb{R}^d$ that initially contains no spheres. If an attempted insertion at time t overlaps with an existing sphere, it is rejected, and additional attempts are made until a nonoverlapping placement is possible. The process can be halted at any finite t, yielding an RSA configuration with a time-dependent packing fraction $\phi(t)$. However, this packing fraction cannot exceed the maximal saturation value $\phi_s = \phi(\infty)$, which is approached in the infinite-time and thermodynamic limits. A packing is saturated if there is no available space to add another nonoverlapping particle to the packing. It is important to emphasize that an RSA packing even at saturation is not jammed.

In the case of 1D RSA packings, also known as the 'car-parking' problem, the saturation packing fraction was obtained analytically[53]: $\phi_s = 0.7475979202....$ However, for $d \geq 2$, ϕ_s in the thermodynamic limit can only be estimated numerically. The most precise numerical study to date[61] has determined $\phi_s = 0.5470735 \pm 0.0000028$ for $d = 2$ and $\phi_s = 0.3841307 \pm 0.0000021$ for $d = 3$. The section 'Sphere packings in high dimensions' reports estimates of ϕ_s in higher dimensions.

One may also ask whether a saturated RSA packing is hyperuniform. A hyperuniform many-particle system in $\mathbb{R}^d$ is one in which long-wavelength density fluctuations are anomalously suppressed compared to typical disordered systems, that is, their structure factors $S(\mathbf{k})$ approach zero as the wavenumber $k \equiv |\mathbf{k}|$ approaches zero[65,66]. In an RSA packing, the pair correlation function $g_2(r)$ decays to unity super-exponentially fast as r becomes large[67], implying that the structure factor $S(k)$ of RSA packings in $\mathbb{R}^d$ is an even and analytic function at zero wavenumber[20,60]. Consequently, saturated RSA packings are not hyperuniform in any finite spatial dimension[60,61]. The nonhyperuniformity of unjammed RSA packings, even at saturation, is expected because hyperuniformity appears to be a signature of jamming in disordered saturated sphere packings, as discussed in greater detail in the subsection 'Jamming categories'.

More generally, a hyperuniform system is defined by a local number variance $\sigma^2(R) \equiv \langle N^2(R) \rangle - \langle N(R) \rangle^2$ associated with the number of particles $N(R)$ within a spherical observation window of radius R that grows slower than window volume or R^d for large R (see refs. 20,65). A volume-growth law is typical of many disordered systems away from critical points, including conventional liquids and structural glasses, not to mention saturated RSA packings. The hyperuniformity concept provides a unified framework to classify perfect crystals and quasicrystals, as well as exotic disordered systems[20,65].

Ghost random sequential addition. Exact results for models of disordered sphere packings across dimensions are rare, but invaluable. In particular, there is a generalization of the RSA process, which can be regarded as a 'thinning' process of a Poisson distribution of spheres, which is parameterized by the positive constant κ that lies in the closed interval [0, 1] (see ref. 68). For $\kappa = 0$, the process reduces to the RSA packings; $\kappa = 1$ corresponds to the 'ghost' RSA process. The ghost RSA model allows for exact determinations of both the time-dependent packing fraction and all n-particle correlation functions g_n for any n and dimension d. In this variant, spheres are placed randomly, irreversibly and sequentially into an initially empty space. However, unlike standard RSA, every rejected sphere is recorded as a ghost sphere, and no further spheres can be added if they would overlap with either an existing or a ghost sphere. The packing fraction at time t for spheres of unit diameter is given by $\phi(t) = [1 - \exp(-v_1(1)t)]/2^d$, where $v_1(1)$ is the volume of a d-dimensional sphere of unit radius. Hence, as $t \to +\infty$, the maximum packing fraction of this d-dimensional unsaturated packing is given by

$$\phi(\infty) = \frac{1}{2^d}, \tag{2}$$

which is substantially smaller than that of the corresponding RSA saturation packing fraction ϕ_s. It is notable, however, that the ghost RSA process is the only hard-sphere packing model that is exactly solvable for all realizable densities and for any dimension. The density scaling shown in equation (2) has implications for the existence of dense high-dimensional disordered packings, as described in the section 'Sphere packings in high dimensions'.

Geometric-structure approach to jammed disordered and ordered packings

Jammed sphere packings are those hard-sphere configurations, ordered or disordered, in which each sphere is in contact with its nearest neighbours such that mechanical stability of a specific type is conferred to the packing, as rigorously defined below. Their structural and physical properties have received great attention, both experimentally and theoretically[16,20,69]. Two powerful and complementary conceptual approaches have emerged to study disordered jammed sphere packings. One approach, motivated by work[70,71] on 'random close packing' (RCP)[72–79], is the long-standing 'ensemble' approach[16,26,80–90] that aims to understand 'typical' (most probable) disordered configurations for a given packing protocol. A notable example is the Edwards generalization of Gibbs–Boltzmann statistical mechanics to treat jammed nonequilibrium granular matter via a volume ensemble of equiprobable jammed states to estimate entropy and 'compactivity' (analogue of temperature)[80,82], which has led to many important developments and predictions[26,83,89]. Another productive outgrowth of the ensemble-average approach is the unifying notion of the jamming phase diagram[81], which extends jamming to include not only granular materials but also glasses formed by supercooling liquids, and which inspired numerous fruitful developments (see refs. 24,91,92 and references therein).

Another approach to jamming, which is emphasized in this Review, is the geometric-structure formalism[17,51,66,69,93–97], which stresses the quantitative description of single-packing configurations (disordered or not), without regard to their frequency of occurrence in the algorithmic or experimental procedure used to generate them. Thus, the geometric-structure approach is broader than the ensemble-average procedure in that it allows the analysis and classification of a single jammed or unjammed packing across the order–disorder spectrum at any achievable packing fraction ϕ, because its probability of occurrence (rare or not) is irrelevant.

At the turn of the twenty-first century, the commonly held view of the RCP state was that it represented the highest possible density achievable by a large collection of disordered identical spheres. However, it was then argued[51] that this concept is ill-defined because the terms 'random' and 'close-packed' were never rigorously defined and are, in fact, conceptually conflicting: close packing implies high coordination (as seen in fcc lattices), which is inherently not random. It was, therefore, proposed to replace the RCP notion with the MRJ state, defined as the most disordered configuration (as measured by an order metric) among all strictly jammed sphere packings in $\mathbb{R}^d$. Thus, the MRJ state under the strict-jamming condition is a prototypical

glass[98] because it is maximally disordered without any long-range order (that is, an infinite set of Bragg peaks), maximally non-ergodic (permanently trapped in configuration space), and perfectly rigid (that is, elastic moduli are unbounded[17,95]).

Jamming categories. For a finite packing of N spheres that exactly obey the impenetrability constraint within some volume in $\mathbb{R}^d$ with a sufficiently smooth boundary, three broad and mathematically precise jamming categories have been defined in order of increasing stringency (mechanical stability)[17,93,95]. In local jamming, each sphere is individually trapped by its neighbours, requiring contact with at least $d+1$ other spheres that are not all confined to the same hemisphere. Next, collective jamming is a locally jammed configuration in which no subset of spheres can be collectively displaced in a way that would allow its members to lose contact with each other or with the rest of the packing. (Collective jamming in hard-sphere packings corresponds to having no 'soft modes' in soft-sphere systems[86,87]). Finally, the most stringent category is strict jamming, which refers to any collectively jammed configuration that prohibits all uniform volume-nonincreasing deformations of the system boundary.

These hierarchical jamming categories closely correspond to the concepts of 'rigid' and 'stable' packings in the mathematical literature[99] and imply the absence of rattlers (that is, particles that are movable but caged) within the packing. The jamming category of a given packing depends on the boundary conditions used (periodic or hard-wall, for example)[17,93,100]. For instance, in $\mathbb{R}^2$, the square-lattice packing with square hard-wall boundary conditions is only collectively jammed (not strictly jammed), but it is only locally jammed (not collectively jammed) under periodic boundary conditions (see refs. 17,93 for lists of the jamming categories of common 2D and 3D crystal packings). Rigorous and efficient linear programming algorithms have been devised to determine whether a given sphere packing is locally, collectively or strictly jammed[96,101].

Jammed packings of N spheres that have the minimal number of contacts required for a jamming category are known as isostatic[100]. In the large-N limit, an isostatic strictly jammed packing has a mean contact number per particle (also known as the kissing number), $Z=2d$ (refs. 100,102). Packings having more contacts than isostatic ones are hyperstatic, whereas those with fewer are hypostatic. Hypostatic sphere packings cannot be collectively or strictly jammed[103], but they may still be locally jammed.

In the vicinity of a jammed state in $\mathbb{R}^d$ with packing fraction ϕ_J, the set of allowed particle displacements converges to a convex-limiting polytope in configuration space because the impenetrability constraints become linear[30,100,104]. According to free-volume theory, the pressure p in this regime has the following exact asymptotic form:

$$\frac{p}{\rho k_B T} \sim \frac{d}{1-\phi/\phi_J} \qquad (\phi \to \phi_J), \tag{3}$$

which enables one to estimate ϕ_J accurately of a given packing, even if the actual jamming point has not quite yet been reached, just by measuring the pressure and extrapolating to $p=+\infty$. The extremely narrow connecting filaments that in principle connect the jamming neighbourhoods[30,100,104] have so little measure that they do not overturn the free-volume leading behaviour of the pressure, even in the infinite-system limit[17]. Although there is no rigorous proof yet for this claim, all numerical evidence strongly suggests that it is correct as the jamming state is approached either along the crystal[30,104] or metastable branches[100] (Fig. 1).

Assuming that the system dynamics remain ergodic in the vicinity of a jammed state, one can apply the fluctuation–compressibility relation[18] along with the free-volume form (equation (3)) to yield the corresponding asymptotic relation for the inverse of the structure factor at the origin[105]:

$$S^{-1}(0) \sim \frac{d}{(1-\phi/\phi_J)^2} \qquad (\phi \to \phi_J). \tag{4}$$

Hence, it is seen that in the limit $\phi \to \phi_J$, the system becomes perfectly hyperuniform. This result appears to validate a more general conjecture[65] that infinitely large packings of identical frictionless hard spheres that are saturated and strictly jammed are hyperuniform, whether ordered or disordered[65]. The subsection 'Order maps' provides an example of a disordered packing that obeys this conjecture.

In the vicinity of a jammed isostatic state, the aforementioned polytope description has been used[100] to derive an exact expression for the probability distribution $P(f)$ of the time-averaged interparticle forces f (under molecular dynamics) that is rigorously linked to the 'quasi-contact' (spheres nearly in contact) behaviour of the pair correlation function $g_2(r)$:

$$\frac{g_2(\epsilon)}{g_2(D^+)} = \int_0^\infty fP(f)\exp(-fp\epsilon), \tag{5}$$

where $\epsilon = r/D - 1 > 0$ is small and p is the pressure.

Order metrics. The geometric-structure approach requires quantification of the degree of 'randomness' or disorder of a packing. A system of N particles is completely characterized statistically by its N-body probability density function $P(\mathbf{R})$ that is associated with finding the N-particle system with configuration $\mathbf{R}$. However, in practice, for large N, $P(\mathbf{R})$ is unavailable. Instead, one must settle for reduced information, such as a scalar order metric $\psi(\mathbf{R})$ that is a well-defined function of a configuration $\mathbf{R}$ with the following two basic properties: it is subject typically to the normalization $0 \le \psi(\mathbf{R}) \le 1$, and, for any two configurations, ψ is larger for the configuration considered to be more ordered[17].

What are the characteristics of a good order metric? It has been suggested that it should have the following additional properties[17,94]: sensitivity to all forms of ordering without bias towards a reference structure; the ability to reflect the hierarchy of ordering between prototypical systems consistent with physical intuition (for example, perfect crystals with high symmetry should exhibit a high degree of order, followed by quasicrystals, then correlated disordered packings without long-range order, and finally uncorrelated particles); the ability to account for both the variety of local coordination patterns and their spatial distribution; and the capability to detect both translational and orientational order across all length scales. Additionally, any useful set of order metrics should yield results that are positively correlated with one another[12,51].

Although there is no perfect order metric, many practically useful scalar ones have been devised and applied to characterize packings, including bond-orientational order metrics in 2D[106] and 3D[37,107,108], translational order metrics[51,94,109,110] and hyperuniformity order metrics[65,111]. Order metrics and maps have been successfully extended to quantify the degree of structural order in condensed phases wherein the constituent particles — whether jammed or not — interact through both attractive and repulsive forces. These extensions encompass models of

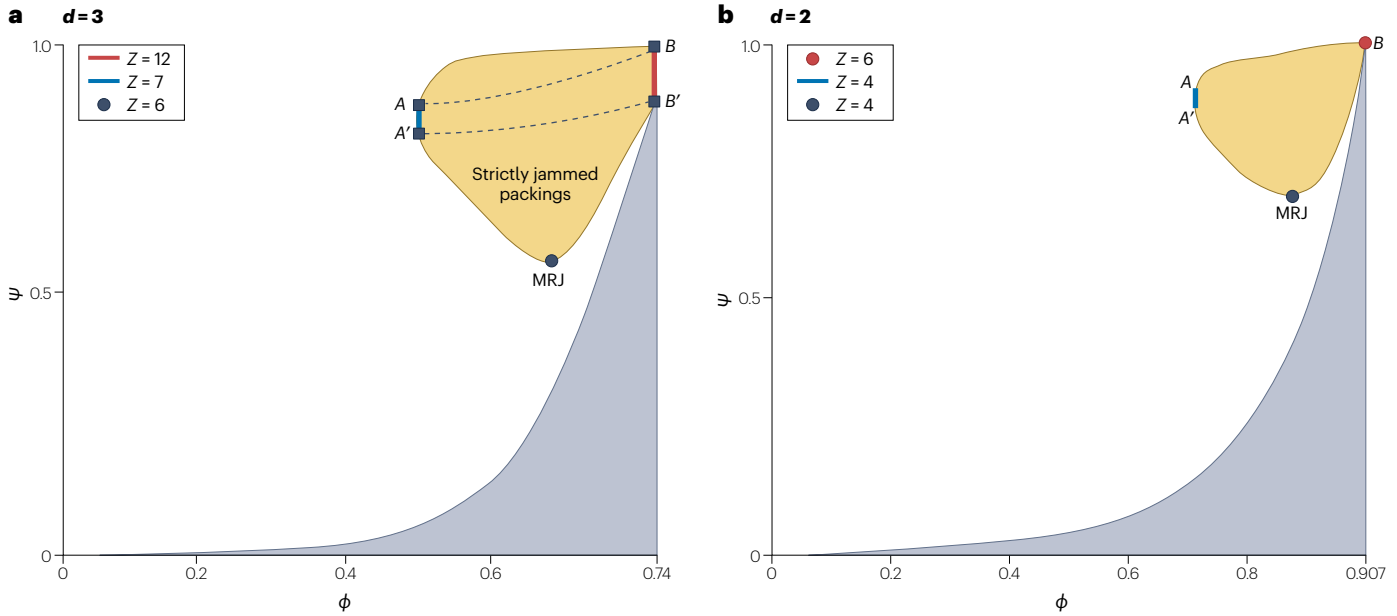


Fig. 2 | Order map of packings of identical spheres in $\mathbb{R}^3$ and $\mathbb{R}^2$ in the density–order (ϕ–ψ) plane. White and yellow regions contain the attainable packings, the yellow region defines the strictly jammed subspaces, and the grey region contains no attainable packings. The boundaries of the jammed region delineate extremal structures. **a**, Map for $\mathbb{R}^3$. The locus of points A–A' corresponds to the lowest-density jammed packings, which in $\mathbb{R}^3$ have density $\phi = 2\pi/(3\sqrt{18}) = 0.49365\ldots$ and kissing number $Z = 7$, known as 'tunnelled crystals'. The locus of points B–B' corresponds to the densest jammed packings, which in $\mathbb{R}^3$ have $\phi = \pi/\sqrt{18} = 0.74048\ldots$ and $Z = 12$, and which are strictly jammed[93,96]. Point B corresponds to the face-centred-cubic (fcc) packing, and point B' represents the most disordered subset of the stacking variants of the fcc structure. Point MRJ represents the maximally random jammed state, that is, the most disordered strictly jammed packing, with $\phi \approx 0.64$ and $Z = 6$. **b**, Order map for $\mathbb{R}^2$. The locus of points A–A' corresponds to the lowest-density jammed packings with $\phi = 3\pi/(8\sqrt{3}) = 0.68017\ldots$ and $Z = 4$. Point B corresponds to the unique densest jammed packing (triangular lattice), with $\phi = \pi/\sqrt{12} = 0.906989\ldots$ and $Z = 6$. Point MRJ represents the maximally random jammed state, that is, the most disordered strictly jammed packing, with $\phi \approx 0.84$ and $Z = 4$. Part **a** reproduced from ref. 20, with the permission of AIP Publishing. Part **b** adapted with permission from ref. 141, PNAS.

simple liquids, glasses and crystals with isotropic interactions[112], amorphous polymers[113], water[114–116] and disordered ground states arising from long-ranged isotropic pair potentials[110].

There are promising order metrics that have yet to be applied to jammed packings, including the τ order metric[110], information content of compressed data files[117], and the local number variance $\sigma^2(R)$ (ref. 118). The τ order metric provides an integrated measure of translational order across length scales[110] and, usefully, has both a direct-space and Fourier-space representation:

$$\tau = \frac{1}{D^d}\int_{\mathbb{R}^d}[g_2(\mathbf{r})-1]^2 d\mathbf{r} = \frac{1}{(2\pi)^d D^d}\int_{\mathbb{R}^d}[S(\mathbf{k})-1]^2 d\mathbf{k}, \qquad (6)$$

where D is a characteristic microscopic length scale. Deviations of the pair functions from unity, whether positive or negative correlations, are picked up by τ, which has been fruitfully applied to describe a broad spectrum of disordered and ordered many-particle systems[110,119–122].

The length of a losslessly compressed data file has also been proposed to measure the degree of order in general many-body systems[117]. The more ordered the system is, the lower is its information content, that is, the shorter the length of its compressed data file. Data compression files of systems in both discrete and continuous spaces have been examined. In the latter case, the coordinates of the system must be discretized, for example, by choosing a grid size such that there is at most one particle centre in each bin, which necessarily introduces some errors. More recently, the local number variance $\sigma^2(R)$ associated with a spherical window of radius R has been shown to provide a sensitive measure of the degree of order, across length scales, of a wide class of point configurations that span from hyperuniform to nonhyperuniform across space dimensions[118].

Order maps. Order maps provide a simple but powerful means to characterize the spectrum of packing states by specifying their order metrics as a function of other packing characteristics. The simplest order map takes any hard-sphere configuration — whether jammed or not — to a single point in the ϕ–ψ plane. Although this two-parameter description captures only a small subset of the relevant parameters needed to fully characterize a packing, it yields useful insights. For example, in $\mathbb{R}^3$, such an order map (Fig. 2a) distinguishes strictly jammed packings[51,94,96,98] from non-jammed packings. (The reader is referred to ref. 17 for analogous order maps for local and collective jamming. There are local jammed states in which the packing fraction is arbitrarily close to zero[13,31].) The boundaries of the jammed region in Fig. 2a delineate extremal structures (Fig. 3). The densest sphere packings[123], with $\phi_{max} = \pi/\sqrt{18} = 0.74048\ldots$, are strictly jammed[93,96]. Of these densest packings, the most ordered and symmetric is the fcc packing. Other stacking variants of the fcc structure are more disordered (see 'Densest packings' subsection). The least dense strictly jammed packings are conjectured to be the so-called tunnelled crystals with $\phi_{min} = 2\phi_{max}/3 = 0.49365\ldots$ (ref. 98). They are subsets of the densest packings but are permeated by infinitely long chains of particle

vacancies[98]. Every sphere in such packings contacts seven immediate neighbours. Remarkably, the tunnelled crystals lie at the threshold of mechanical stability: removing even a single interior sphere leads to the collapse of the entire packing. Importantly, among the set of all packings at the same density, tunnelled crystals form a set of zero measure and are, thus, virtually impossible to discover using conventional packing algorithms. The existence of such structures highlights the importance of analysing individual packings, regardless of their frequency of occurrence in the space of jammed configurations — an approach advocated by the geometric-structure perspective.

Before discussing the 3D MRJ state, a configuration of which is shown in Fig. 3b, it is useful to describe the analogous states in the 2D order map for identical hard circular disks corresponding to the lowest-density jammed packing and most ordered, highest-density jammed packing, respectively (Fig. 2b). In $\mathbb{R}^2$, the strictly jammed triangular lattice with $\phi_{max} = \pi/\sqrt{12} = 0.90689\ldots$ and $Z = 6$ is the unique densest packing[124], corresponding to the single point B, in contrast to the line B-–B' of the densest sphere packings in the order map for $\mathbb{R}^3$. In 2D, point A corresponds to the 'reinforced' kagome packing with precisely four contacts per particle, and $\phi_{min} = 3\pi/(8\sqrt{3}) = 0.68017\ldots$ in the infinite-volume limit. This packing is putatively the lowest density strictly jammed subpacking of the triangular-lattice packing that has the highest degree of order[96]. It is noteworthy that this packing has the isostatic contact number per particle of $Z = 4$ and yet is an ordered packing, which runs counter to the prevailing notion that isostaticity is a consequence of 'genericity' or randomness[102]. Point A' allows for the possibility that there exist other least dense strictly jammed packings with the same packing fraction as the reinforced kagome packing but with a lower order metric. We know that there are other such related packings with the isostatic value of $Z = 4$, but with less symmetry[93]. I remark on the 2D MRJ state below.

Among all strictly jammed sphere packings in $\mathbb{R}^d$, the MRJ state is that which exhibits the greatest degree of disorder, that is, it minimizes some given order metric ψ (ref. 51) (Fig. 2). This minimal state is well-defined in the sense that the degree of order along the lower jammed boundary must increase when an increase in Z from the isostatic value of 6 results from transitioning from the MRJ state towards either the maximum packing density (fcc and its stacking variants) or the minimum density consistent with strict jamming (tunnelled crystals); thus, any useful order metric rises on either side of the MRJ state[97]. Various well-founded order metrics consistently identify a 3D MRJ state with a packing fraction $\phi_{MRJ} \approx 0.64$ (see ref. 94), which approximately matches the traditionally accepted density estimates of the RCP state obtained either by experimental[72], numerical[76,77] or theoretical methods[27,42,89]. That different order metrics identify the same MRJ density speaks to their utility and robustness, despite the absence of a universally perfect order metric. Furthermore, it is important to note that the packing fraction alone does not fully characterize the MRJ state. At this same density, it is possible to have strictly jammed packings that are substantially more ordered[94] (Fig. 2).

The original Lubachevsky–Stillinger molecular-dynamics packing algorithm[125] was refined[126] and then applied[100,127] to generate 3D MRJ-like states and to study their pair statistics (without removal of a small concentration of rattlers). The computed pair correlation function for such packings exhibits (in addition to the Dirac-delta-function peak at contact) the well-known split second peak (common to disordered isostatic packings[128]) and an integrable power-law divergence $g_2(r) \sim (r/D - 1)^{-\gamma}$ with a 'gap' exponent $\gamma \approx 0.4$ for near contacts[100] (Fig. 4a).

In a million-particle MRJ-like saturated packing generated by the same packing algorithm, the structure factor $S(k)$ approaches zero (within numerical error) as k approaches zero (Fig. 4b), and hence, MRJ states are effectively hyperuniform, which supports the general conjecture of ref. 65 noted earlier. This hyperuniform behaviour, which appears to be a signature of jamming in disordered and saturated packings of identical spheres, has been verified elsewhere[129–132]. (Hyperuniformity is also putatively a signature of jamming in disordered saturated packings of spheres with a polydispersity in size[133].) Existing algorithms that produce disordered jammed packings inevitably contain a small fraction (1.5–3%) of rattlers, which are defects that degrade perfect hyperuniformity. Perfect hyperuniformity $[\lim_{k\to 0} S(k) = 0]$ can only be achieved in the ideal MRJ state, which is rattler-free, as suggested by free-volume theory[105] (see the discussion in the subsection 'Jamming categories', after equation (4)). It is noteworthy that a nearly hyperuniform system possesses a hyperuniform scaling regime over a finite range of length scales before turning over to a nonhyperuniform scaling regime, as measured by the local number variance $\sigma^2(R)$ (ref. 105). Thus, one can use the evaluation of the variance as function of R as a rough diagnostic of how close a disordered saturated packing is to jamming by determining the range of the hyperuniform scaling regime.

Three-dimensional disordered isostatic jammed states of identical frictionless spheres[51,69,127,131,134–136] have been numerically created to

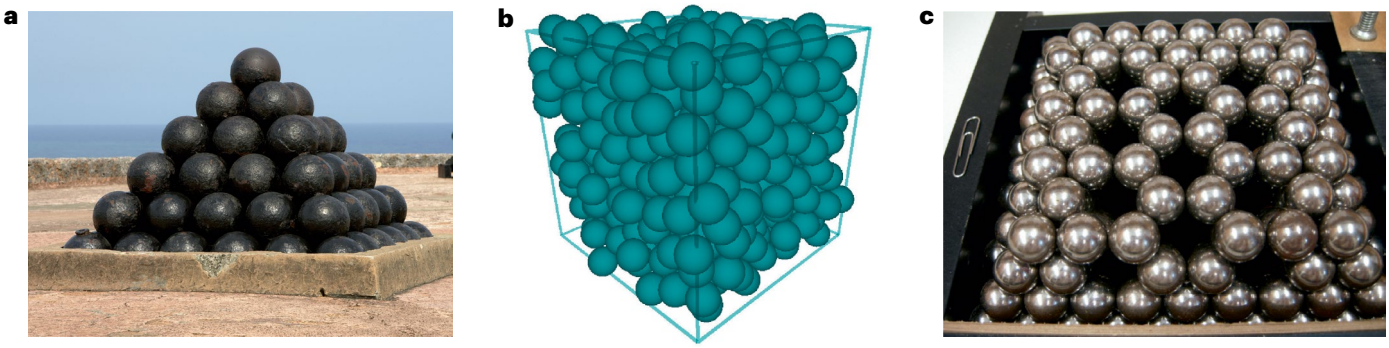


Fig. 3 | Three different extremal strictly jammed packings in $\mathbb{R}^3$. The packings are identified in the order map shown in Fig. 2. **a**, Face-centred cubic packing with density $\phi = \pi/\sqrt{18} = 0.74048\ldots$ and kissing number $Z = 12$ (hyperstatic). **b**, Maximally random jammed packing with $\phi \approx 0.64$ and $Z = 6$ (isostatic). **c**, A tunnelled crystal with $\phi = 2\pi/(3\sqrt{18}) = 0.49365\ldots$ and $Z = 7$ (hyperstatic). Part **a** is adapted with permission from Franz Marc Frei (The Image Bank Unreleased/Getty). Parts **b** and **c** are reprinted with permission from ref. 17, APS.

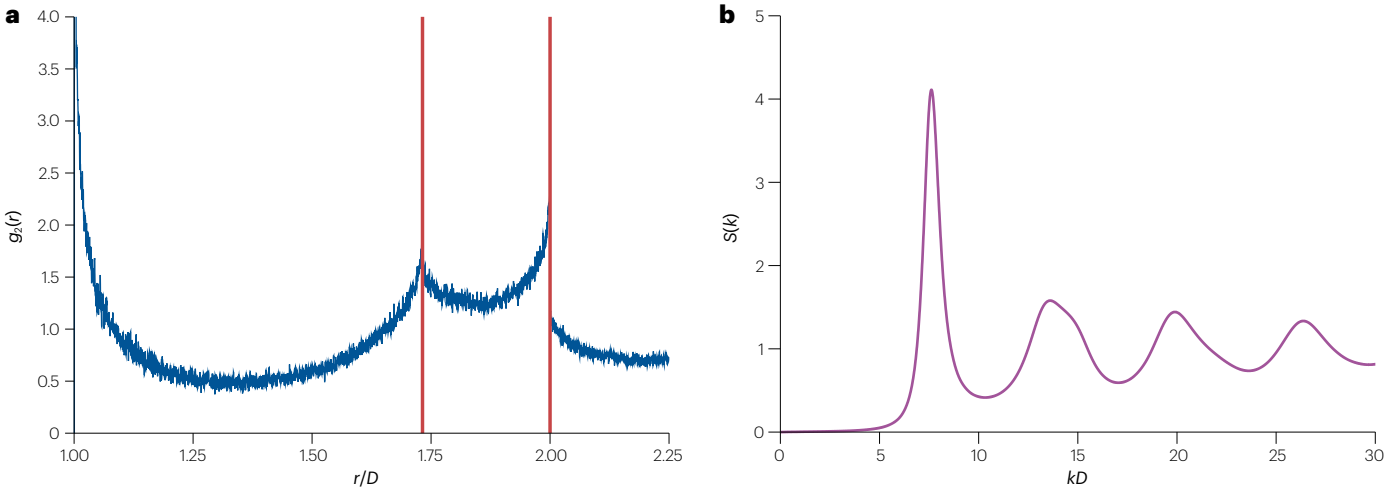


Fig. 4 | Pair statistics of the 3D MRJ state. a, Pair correlation function $g_2(r)$ versus dimensionless distance r/D (where D is sphere diameter) for the 3D maximally random jammed (MRJ) state with density $\phi \approx 0.64$ (ref. 100). **b**, The corresponding structure factor $S(k)$ versus dimensionless wavenumber kD (ref. 127).

good approximation by various protocols under periodic boundary conditions, including rapid compression of hard spheres[69,126,127,131,135] to their deep mechanically stable local 'energy' ($-\phi$) minima (inherent structures[69,137]), rapid quenching of soft spheres at high T to find inherent structures at $T = 0$ via conjugate gradient techniques[134,135], or as a dynamical phase transition via a biased random organization protocol[129]. Different packing protocols lead to 3D disordered isostatic jammed packings with similar but not exactly the same structural features, such as packing fractions, rattler concentrations, gap exponents, force distributions and large-scale density fluctuations. For example, the Torquato–Jiao linear programming algorithm[69], which is designed to yield strictly jammed packings, produces 50% fewer rattlers[136] than does the modified Lubachevsky–Stillinger algorithm[100,126]. The so-called weak-force scaling law $P(f) \sim f^{\theta}$ is obtained from the force distribution defined in equation (5), in the limit $f \to 0$. Stability requires an inequality between θ and the aforementioned gap exponent γ, namely, $\gamma \geq 1/(2+\theta)$ (ref. 138) (see ref. 139 for another derivation). Numerical estimates for the exponent θ for hard spheres have been reported in the range 0.2 – 0.28 (refs. 135,138). It is noteworthy that 3D disordered sphere packings have been generated that are exactly hyperuniform in the degenerate 'stealthy' hyperuniform ground-state manifold (associated with certain soft long-ranged interactions) that are remarkably configurationally extremely close to hyperuniform 3D MRJ sphere packings[140].

MRJ compared to RCP states

The MRJ state refers to a unique infinite packing that is maximally disordered while satisfying the strict jamming constraint, independent of how probable it is to occur in a particular packing protocol. Consequently, the MRJ state is conceptually and quantitatively different from RCP packings[3,70,71], which, more recently, have been reasonably suggested to be the most probable jammed packings associated with an ensemble[85]. Whereas numerically generated MRJ states have similar packing fractions as RCP states in 3D ($\phi \approx 0.64$) and have similar pair statistics, they are distinctly different in 2D for monodisperse circular-disk packings, including their respective densities, average contact numbers, and degree of order[141]. Dense 2D monodisperse (circular) disk packings (unlike their 3D counterparts) are not geometrically frustrated, that is, the densest local packing arrangement is compatible with the globally densest packing arrangement (the triangular lattice). Consequently, standard packing protocols have difficulty generating disordered, jammed packings of monodisperse disks, resulting instead in a polycrystalline hyperstatic arrangement – an outcome that challenges the notion of these being true MRJ states.

The identification of truly disordered, isostatic jammed disk packing has remained elusive largely because they become sets of zero measure as the system size increases, and hence, standard algorithms had not been able to suggest their existence. Using the Torquato–Jiao algorithm and the geometric-structure approach, moderately large 2D MRJ-like identical disk packings with $\phi \approx 0.83$ were generated and analysed, which were not polycrystalline; rather, they were isostatic and substantially more disordered, as measured by bond-orientational and translational order metrics[141]. A subsequent theoretical study[142], which used the geometric-structure approach to obtain a closed-form formula for the packing fraction of 2D isostatic MRJ monodisperse disks, predicts $\phi = 0.834$, which is in very good agreement with the numerical value found in ref. 141.

Densest packings

The sphere packing problem seeks to answer the following questions: Among all packings of congruent spheres in $\mathbb{R}^d$, what is the maximal packing fraction ϕ_{max}? What are the corresponding arrangements of the spheres[8]? The optimal solutions in 1D and 2D correspond to the integer-lattice packing with $\phi_{max} = 1$ and triangular-lattice packing with $\phi_{max} = \pi/\sqrt{12} = 0.9068\ldots$ (ref. 124), respectively. (The term 'lattice' refers here to a Bravais lattice only, that is, one that has one lattice site per unit cell.) In the case of $d = 3$, these questions were asked in 1611 by Kepler, who sought the densest way to stack equal-sized cannon balls? He conjectured that the fcc lattice is the best arrangement. In 2005, Kepler's conjecture was proved[123] by showing that there is no other arrangement of spheres in $\mathbb{R}^3$ whose density can exceed that of the fcc-lattice packing and, hence, $\phi_{max} = \pi/\sqrt{18} = 0.7404\ldots$ (see also ref. 1 for a popular account of the proof). Note that for $d = 3$, there is an

uncountably infinite number of non-lattice packings (called Barlow packings[143]) that have the same density as the densest fcc packings. A periodic packing of spheres is an arrangement of N nonoverlapping spheres within a fundamental cell of a lattice, which is then periodically replicated, and hence is a non-lattice (non-Bravais lattice) packing when $N \geq 2$.

Sphere packings in high dimensions

Physicists have studied disordered sphere packings in dimensions greater than three to gain insight into liquid, metastable and glassy states of matter, as well as to infer disordered phase behaviour in lower dimensions[16,25,131,135,144–150]. The study of the large-d limit has been shown to be a fruitful device, as in other areas of physics. The densest sphere packings in high dimensions, which may or may not be ordered, are of great interest to physicists and mathematicians. Remarkably, the optimal way of sending digital signals over a noisy communication channel corresponds to the densest sphere packing in a high-dimensional space[4] (see also ref. 8). These 'error-correcting' codes underpin many digital communication and storage systems, including compact discs, cell phones and the Internet.

It is instructive here to introduce the decorrelation principle[151]. This is the principle that in disordered sphere packings, unconstrained correlations vanish asymptotically in high dimensions, and the n-particle correlation functions, g_n for any $n \geq 3$, can be inferred entirely (up to small errors) from a knowledge of ρ and the pair correlation function g_2. The decorrelation principle operates for all of the disordered packing models described below, even as the dimension increases for relatively small d. Interestingly, the decorrelation principle has been generalized to apply to periodic packings with high symmetry and, hence, those with long-range order[152,153].

Equilibrium and metastable packings

The study of equilibrium and metastable states of hard spheres in spatial dimensions greater than three has received considerable theoretical and computational attention over the years[144,145,154–159]. This includes the evaluation of various virial coefficients across dimensions[154,156,160], the determination of the pressure along the liquid, metastable and crystal branches[145,155,157–162], and the determination of the pair correlation functions and structure factors along the liquid and metastable branches[145,162,163]. Note that for any d-dimensional disordered packing in which the pair correlation function at contact, $g_2(D^+)$, is bounded (including equilibrium and metastable configurations away from jammed states), the structure factor $S(k)$ has a power-law tail in the limit $k \to \infty$ of the form $k^{-(d+1)/2}$ (see ref. 105 for the exact asymptotic formula). The freezing and melting packing fractions, ϕ_F and ϕ_M, respectively, associated with the equilibrium hard-sphere fluid–solid transition have been estimated using a modified Lubachevsky–Stillinger packing algorithm[145]. For $d = 4$, $\phi_F \simeq 0.32$ and $\phi_M \simeq 0.39$; for $d = 5$, $\phi_F \simeq 0.19$ and $\phi_M \simeq 0.24$. These results indicate that crystal nucleation is increasingly suppressed as dimension grows (see also ref. 158). Additionally, a variety of approximate theoretical methods have been used to demonstrate that hard spheres in equilibrium undergo a first-order freezing transition, even in dimensions as high as $d = 50$ (ref. 155).

Concerning the fate of hard-sphere crystallization in high dimensions, three simple possible scenarios[164] are as follows: crystallization is hindered, making the glass phase the densest packing; crystallization from the liquid can occur but only well beyond the dynamical glass transition, rendering it improbable to happen dynamically; and crystallization is possible and occurs before or just after dynamical arrest, thus making it realistically accessible from the liquid state. It has been suggested that the third scenario is most probable based on numerical simulations in relatively low dimensions ($d = 3$–10) and cell-cluster expansions[164]. If 'crystallization' in this scenario allows for a periodic structure with ever increasing complexity as d approaches infinity and, hence, effectively disordered packings, then this outcome would be consistent with the conjecture that the densest packings in the high-d limit are effectively 'disordered'[151], which is discussed below.

Unjammed nonequilibrium packings

Ghost random sequential addition. As noted earlier, the maximal packing fraction of an unsaturated and disordered ghost RSA packing in any d, given by $1/2^d$ (see equation (2)), is asymptotically equivalent to Minkowski's lower bound on the maximal packing fraction ϕ_{max} for Bravais lattices (see lower bound shown in equation (8)). This exact result for unsaturated and unjammed packings suggested that disordered packings might be denser than lattice packings in high dimensions[68]. Note that unlike standard unsaturated RSA packings, for ghost RSA packings, the pair correlation function at contact, $g_2(D^+)$, is bounded. The ghost RSA packing vividly manifests the above-mentioned decorrelation principle, even in relatively low dimensions, implying that $g_2(r)$ approaches the step function $\Theta(r - D)$ as $d \to \infty$.

Random sequential addition. For dimensions four, five and six, pair statistics (pair correlation functions and structure factors) have been computed for numerically generated saturated RSA sphere packings[60]. A more efficient and precise numerical protocol was formulated to produce such saturated packings for dimensions up to eight[61]. The current best estimates of the maximal saturation packing fraction ϕ_s for $d = 4, 5, 6, 7$ and 8 are 0.2600781 ± 0.0000037, 0.1707761 ± 0.0000046, 0.109302 ± 0.000019, 0.068404 ± 0.000016 and 0.04230 ± 0.00021, respectively[61]. These are lower than the corresponding MRJ packing fractions in those dimensions, as described below. In the large-d limit, theoretical considerations[165] suggest that the high-dimensional scaling of the saturation packing fraction ϕ_s is of the form

$$\phi_s \sim \frac{d \ln(d)}{2^d}. \tag{7}$$

The pair correlation function of saturated RSA configurations has a logarithmic singularity as the pair distance approaches the contact value, that is, $g_2(r) \sim a_0 \ln(r/D - 1)$ in the limit $r \to D^+$ (refs. 57,166). For $d \geq 3$, the coefficient a_0 diminishes as d increases[61]. Although saturated RSA packings are nearly but not exactly hyperuniform[60], as d increases, the degree of hyperuniformity increases, and pair correlations markedly diminish[61], consistent with the decorrelation principle[151] mentioned above.

Jammed disordered and ordered packings

Disordered jammed states. Estimations of the packing fractions for MRJ packings generated using the modified Lubachevsky–Stillinger algorithm are $\phi_{MRJ} \simeq 0.46$, 0.31 and 0.20 for $d = 4$, 5 and 6, respectively, which, to a good approximation, obeys the scaling form $\phi_{MRJ} = c_1 2^{-d} + c_2 d \cdot 2^{-d}$, where $c_1 = -2.72$ and $c_2 = 2.56$ (ref. 145). This low-d behaviour is consistent with high-dimensional asymptotic scaling $d \cdot 2^{-d}$, which is supported by theoretical studies[90,139,151,167]. The fraction of

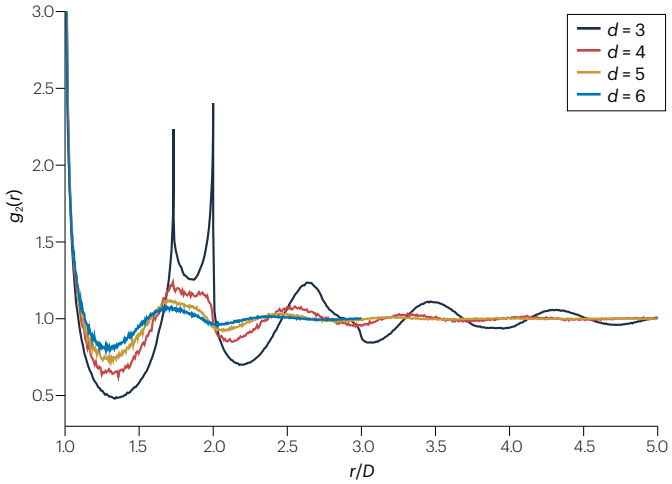


Fig. 5 | Pair correlation function $g_2(r)$ versus dimensionless distance r/D (where D is sphere diameter) for MRJ sphere packings in dimensions $d = 3$, 4, 5 and 6. Spatial correlations are clearly seen to diminish as the space dimension increases, consistent with the decorrelation principle[151].

rattlers (defects) decreases substantially as d increases. In addition, the MRJ pair correlation function $g_2(r)$ and structure factor $S(k)$ for these states indicate that short-range ordering appreciably decreases with increasing dimension[145], consistent with the decorrelation principle[151] (Fig. 5). This result implies that, in the limit $d \to \infty$, $g_2(r)$ approaches unity for all r outside the hard core, except at contact wherein the jamming constraint results in a Dirac delta function, leading to the density scaling $d/2^d$ (refs. 151,167). As was the case for $d = 3$ (where $\phi_{\mathrm{MRJ}} \simeq 0.64$), the MRJ packings in higher dimensions were found to be isostatic and hyperuniform with a power-law divergence in $g_2(r)$ of near contacts, that is, $g_2(r) \sim 1/(r-D)^{\gamma}$ with $\gamma \approx 0.4$ as r approaches D^+. Note that for any d-dimensional disordered packing in which the pair correlation function possesses a single Dirac delta function at contact, the structure factor $S(k)$ exhibits a power-law tail in the limit $k \to \infty$ of the form $k^{-d/2+1}$ (see ref. 105 for the exact asymptotic formula).

Simulations[135] of disordered jammed packings in dimensions up to ten, using a variety of protocols, confirm many of the results reported in ref. 145 for $d = 4$, 5 and 6. In addition, theoretical analyses in ref. 135 show that the quasi-contact regime and 'weak-force' distribution for a variety of different isostatic jammed packings are characterized by very similar scaling behaviours.

For MRJ states in dimensions $d = 3$, 4 and 5, generating high-quality strictly jammed states is crucial for ensuring hyperuniformity and accurately extracting the hyperuniformity exponent $\alpha > 0$ (ref. 131). (This exponent is defined by the power-law behaviour of $S(\mathbf{k}) \sim |\mathbf{k}|^{\alpha}$ as $|\mathbf{k}|$ approaches zero.) Additionally, for fixed d, as the particle number N increases, it is more difficult to ensure that the generated states are jammed, resulting in packings that are nonhyperuniform. Analysis of the largest high-quality jammed packings suggests that the ideal MRJ packings for all dimensions $d \geq 3$ are hyperuniform with $\alpha = d - 2$, demonstrating that the packings become increasingly more hyperuniform as d increases. The differences in α between MRJ packings and the proposed Manna-class RCP states[129], which were reported to have $\alpha = 0.25$ in $d = 3$ and be nonhyperuniform ($\alpha = 0$) for $d = 4$ and $d = 5$, demonstrate the vivid distinctions between the large-scale structure of RCP and MRJ states in these dimensions.

The replica theory for glasses and jamming[16,25] is a powerful mean-field theory that applies in the limit of infinite dimensions owing to the aforementioned decorrelation principle. Accordingly, mean-field theory results are not guaranteed to be seen in finite dimensions precisely because correlations cannot be neglected. How relevant this description might be for understanding low-dimensional glass-forming liquids, however, remains unclear[149]. Nonetheless, it is remarkable that this theory predicts universal behaviour of jamming exponents associated with quasi-contact and weak-force scalings across dimensions that are accurate, even in finite dimensions ($d \geq 2$)[16,25,148].

Densest packings. What is known about the densest sphere packings in dimensions greater than three? For $4 \leq d \leq 9$, the densest known packings are lattice packings[8]. For example, the 'checkerboard' lattice D_d, a d-dimensional generalization of the fcc lattice (densest packing in $\mathbb{R}^3$), is believed to be optimal in $\mathbb{R}^4$ and $\mathbb{R}^5$. In $\mathbb{R}^8$, the unique densest packing is the remarkably symmetric E_8 lattice[168]; in $\mathbb{R}^{24}$, it is the Leech lattice L_{24} (ref. 169). Table 1 lists the densest known sphere packings in $\mathbb{R}^d$ for selected d. It is noteworthy that the non-lattice (periodic) packing P_{10c}, which contains 40 spheres per fundamental cell, is the densest known packing in $\mathbb{R}^{10}$. This dimension is the lowest dimension in which the densest known packing is not a (Bravais) lattice.

The Torquato–Jiao linear-programming packing algorithm[165] has been adapted[170] to find the densest lattice packings up to 19 dimensions. It rapidly and reliably recovered the densest known lattice packings[8] without a priori knowledge of their existence. Subsequently, this algorithm was used to produce an ensemble of isostatic jammed hard-sphere lattices to study the associated pair statistics and force distributions[171]. Importantly, in sufficiently large dimensions, lattices cannot be the densest packings as they are almost surely unsaturated, because holes (space exterior to the spheres) dominate the d-dimensional space[8]. A geometrical constraint satisfaction algorithm has been used to efficiently generate non-lattice sphere packings in dimensions up to 22 (ref. 172). Using this approach, it is computationally easy to double the density of the best-known lower bound (described below) on lattice packings in such dimensions. Furthermore, the exponential decay rate of the packing fraction might be improved relative to Minkowski's lattice sphere packing asymptotic scaling of $1/2^d$ (stated below), which is consistent with the theoretical results reported in ref. 151.

Importantly, it becomes increasingly difficult to find explicit dense packing constructions as d becomes large, not to mention the fact that the problem of finding the shortest lattice vector grows super-exponentially with d and is in the class of nondeterministic polynomial-time complete (NP)-hard problems[173]. For large d, the best one can do to characterize the densest packings theoretically is to devise upper and lower bounds on the maximal packing fraction $\phi_{\max}$ (ref. 8). Among all lattice packings for $d \geq 2$, Minkowski[2] proved the following nonconstructive lower bound:

$$\phi_{\max} \geq \frac{\zeta(d)}{2^{d-1}}, \tag{8}$$

where $\zeta(d) = \sum_{n=1}^{\infty} n^{-d}$ is the Riemann zeta function; thus, this lower bound is controlled by 2^{-d} in limit $d \to \infty$. Note that this density scaling is exactly realized by an explicit disordered packing construction, namely, the aforementioned unsaturated ghost RSA packing in the infinite-time limit[68] (see equation (2)). The existence of this unsaturated and unjammed disordered packing strongly suggests that lattice packings, which become unsaturated for sufficiently large d, are far

Table 1 | Best-known solutions to the sphere packing problem in selected dimensions

Dimension (d)	Packing[a]	Packing fraction (ϕ)	Kissing number (Z)
1	$A_1^* = \mathbb{Z}$	1	2
2	$A_2^* \equiv A_2$	$\pi/\sqrt{12} = 0.906899\ldots$	6
3	$A_3 \equiv D_3$	$\pi/\sqrt{18} = 0.740480\ldots$	12
4	$D_4 \equiv D_4^*$	$\pi^2/16 = 0.616850\ldots$	24
5	D_5	$2\pi^2/(30\sqrt{2}) = 0.465257\ldots$	40
6	E_6	$3\pi^3/(144\sqrt{3}) = 0.372947\ldots$	72
7	E_7	$\pi^3/105 = 0.295297\ldots$	126
8	$E_8 = E_8^*$	$\pi^4/384 = 0.253669\ldots$	240
9	Λ_9	$\sqrt{2}\pi^4/945 = 0.145774\ldots$	272
10	P_{10c}	$\pi^5/3{,}072 = 0.099615\ldots$	372
12	$\Lambda_{12}^{\max}$	$\pi^6/23{,}040 = 0.041726\ldots$	648
16	Λ_{16}	$\pi^8/645{,}120 = 0.014708\ldots$	4,320
24	$\Lambda_{24} = \Lambda_{24}^*$	$\pi^{24}/479{,}001{,}600 = 0.001929\ldots$	196,560

[a]Details are given in ref. 8.

from optimal for large d. Additional evidence for this possibility is provided below.

Since Minkowski's work, many extensions of the lower bound (equation (8)) for lattice packings have been derived[8,174–178], but none of these results improved on the dominant asymptotic exponential term 2^{-d}. The aforementioned lower bounds generally involve an improvement in Minkowski's bound that is linear in d in the limit $d \to \infty$, implying the following asymptotic form:

$$\phi_{\max} \geq c\frac{d}{2^d}, \tag{9}$$

where c, except for very special dimensions, is a constant. For general dimensions, the best lower bound[175] in the high-d limit yields $c = 2$, improving on the value $c = 1.68$ obtained earlier[174]. For dimensions divisible by four[176], the constant c has been further improved[177]. For very special d, the lower bound (equation (9)) can be improved by replacing c by $\ln\ln d$ (ref. 177). Recently, it was proved[179] that there are lattice packings whose packing fraction is at least $cd^2/2^d$, thus providing the first improvement on the bound of ref. 175 by a factor of d.

The existence of disordered packings whose packing fraction obeys the lower bound (equation (9)) with $c = \ln(2/\sqrt{(3)}) = 0.14384\ldots$ has been proved[178]. It is noteworthy that a lower bound on $\phi_{\max}$ has been conjectured[167] that applies to disordered sphere packings of the same asymptotic form as inequality (9) with $c = 0.5$. Furthermore, disordered packings with densities that improve on the asymptotic lower bound (equation (9)) by a factor $\ln(d)$ exist[180]; specifically, the following asymptotic lower bound has been proved:

$$\phi_{\max} \geq \frac{0.5d\ln(d)}{2^d}. \tag{10}$$

Interestingly, the same asymptotic density scaling was estimated to apply to glassy sphere packings[16].

A linear program (LP) was formulated to obtain lower bounds on $\phi_{\max}$ (ref. 167); this procedure was subsequently applied to support the counterintuitive conjecture that, for large-enough d, the densest sphere packings may be disordered, or at least have fundamental cells whose size and structural complexity increase with dimension[151]. Specifically, given a fixed 'test' radial pair correlation function $g_2(r;\mathbf{a})$ for all r that is defined for a prescribed set of parameters $\mathbf{a}$, the LP formulation maximizes the packing fraction ϕ over the parameters $\mathbf{a}$ to yield the range of packing fractions $0 \leq \phi \leq \phi_*$ such that the corresponding structure factor $S(k)$ is nonnegative for all k. When there exist sphere packings with a g_2 satisfying these conditions in the interval $[0, \phi_*]$, then the lower bound on the maximal packing fraction is

$$\phi_{\max} \geq \phi_*. \tag{11}$$

It has been conjectured[151] that a test function $g_2(\mathbf{r})$ is a pair correlation function of a translationally invariant disordered sphere packing in $\mathbb{R}^d$ for $0 \leq \phi \leq \phi_*$ in sufficiently high dimensions if and only if the nonnegativity conditions on $S(\mathbf{k})$ and $g_2(\mathbf{r})$ are met. Using a step function $\Theta(r-D)$ test function, corresponding to a disordered packing with no correlations beyond the hard core, it is easily shown that $\phi_{\max} \geq 1/2^d$ (see refs. 151,167), which, as noted earlier, is exactly achieved by the ghost RSA packing as $d \to \infty$ and is the same scaling as Minkowski's lower bound (equation (8)) for a lattice. An improved lower bound $(d+2)/2^d$, which is of the same form as the rigorous lower bound (equation (9)), was obtained using a test function that is the sum of a step function and a Dirac delta function at contact of arbitrary weight and then optimization[151,167]. A test function $g_2(\mathbf{r})$ corresponding to a disordered sphere packing with additional correlations[151] has been used to find a conjectural lower bound on $\phi_{\max}$ that is controlled by $2^{(\log_2(e)-3)d/2} = 2^{-(0.77865\ldots)d}$, providing the putative exponential improvement of Minkowski's lower bound (equation (8)). The decorrelation principle[151], among other results[17,153,181], provides justification for the conjecture. In fact, there is a wide class of test functions (corresponding to disordered packings) that lead to the same decay rate $2^{-(0.77865\ldots)d}$ (ref. 181), implying that it is a robust result. Figure 6 compares this conjectured LP lower bound for $3 \leq d \leq 36$ to the corresponding LP upper bound described below and the best-known packings. The decay rate has also been recently matched using a completely different

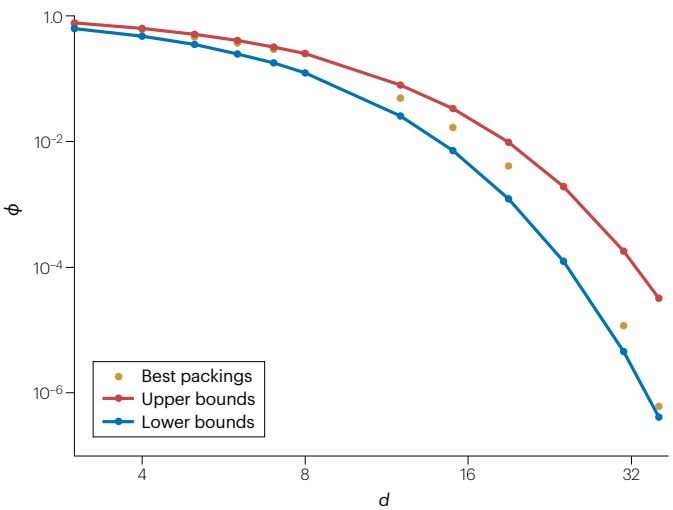


Fig. 6 | Best-known packings in dimensions $3 \leq d \leq 36$ compared to upper and lower bounds on the maximal packing fraction ϕ. The upper bounds are the linear programming upper bounds of ref. 183, and the lower bounds are the conjectured linear programming lower bounds of ref. 181.

approach (particular uncertainty principles of Fourier analysis) to yield the conjectured lower bound on ϕ_{max} (ref. 182).

Interestingly, the optimization problem defined in ref. 167 is the dual of the infinite-dimensional LP devised[183] to obtain upper bounds on ϕ_{max}. Here, one considers a test radial function $f(r)$ in $\mathbb{R}^d$ such that it is nonpositive for $r \le D$ with a Fourier transform $\tilde{f}(k)$ that is nonnegative for all k. Then, the number density ρ is bounded from above by $\frac{\tilde{f}(0)}{2^d f(0)}$. The radial function $f(r)$ can be physically interpreted to be a pair potential. The fact that its Fourier transform must be nonnegative for all k is a well-known stability condition for many-particle systems with pairwise interactions[184]. Every LP has a dual program, and although for any finite-dimensional LP, there is no duality gap between the upper and lower bound formulations, this may not be true for an infinite-dimensional LP. However, recently it has been proved[185] that there is no duality gap for the infinite-dimensional LP bounds.

The LP upper bounds[183] improve on earlier ones[5,186] for all dimensions, and they were used to prove the best-known upper bounds on ϕ_{max} (to that date) for dimensions in the range $4 \le d \le 36$ (Fig. 6). Recently, this LP upper-bound formulation was used to prove that no packings in $\mathbb{R}^8$ and $\mathbb{R}^{24}$ have densities that can exceed those of the E_8 (ref. 168) and L_{24} (ref. 169) lattices, respectively. Three-point upper bounds on the sphere packing density in dimensions 4–7 and 9–16 have been computed[185] using semi-definite programming that improved on the corresponding LP upper bounds. The best-known asymptotic high-d upper bound on the maximal packing fraction is $\phi_{max} \le 2^{-0.5990d}$ (ref. 187). This result proves that the maximal packing fraction approaches zero in this limit. This somewhat counterintuitive high-dimensional property of sphere packings can be understood by recognizing that nearly all of the volume of a d-dimensional sphere for large d is concentrated close to its surface. The scaling of ref. 187 can also be obtained via LP formulations with improved coefficients[188,189], but a fundamental open question is whether LP-type upper bounds can yield improvement on this decay rate. Computations[23] suggest that this may be case, but the improvement in the decay rate is expected to be small.

Outlook

There are many outstanding open questions for future research, which include — but are certainly not limited to — the following list: Can one rigorously prove that there are disorder to order phase transition or transitions of equilibrium (Gibbsian) hard spheres in two, three and higher dimensions? Is it possible to devise an algorithm that produces rattler-free 3D MRJ-like sphere packings? Why does the fraction of rattlers substantially decrease for MRJ packings in larger dimensions and putatively approaches zero for sufficiently large d? Could it be proved that all strictly jammed, saturated packings of identical spheres in $\mathbb{R}^d$ are hyperuniform, as conjectured previously[65]? Is it possible to devise substantially more incisive order metrics to characterize jammed and unjammed packings than those that presently exist? Is it possible to formulate closed-form theoretically based formulas for the packing fraction and, more importantly, the pair statistics of MRJ-like sphere packings in low dimensions that closely match the features seen in computer simulations (Figs. 4 and 5)? Can Ulam's conjecture[190], which posits that the densest packings of identical spheres has a packing fraction that is smaller than that of any other convex body, be proved? There are only five spatial dimensions (namely, $d = 1, 2, 3, 8$ and 24) in which the densest sphere packings have been provably identified. Can the same be done in other dimensions? For example, can one prove that the checkerboard lattice D_4 in $\mathbb{R}^4$ or the E_6 root lattice in $\mathbb{R}^6$ are the densest packings in those dimensions? Could one identify the analogues of the strictly jammed tunnelled crystals[98] (which are at the cusp of stability) in four and higher dimensions? Can lower bounds on the density of the densest lattice packings be devised such that they improve on the asymptotic form $cd^2/2^d$ obtained recently[179]? Is it possible to exponentially improve on the upper bound $\phi_{max} \le 2^{-0.5990d}$ (ref. 187) in the high-d limit? Can it be shown that the densest sphere packings as $d \to \infty$ are 'effectively' disordered? Even partial solutions to the aforementioned challenging problems would be major developments in the physics and mathematics of sphere packings.

Published online: 19 March 2026

References

1. Aste, T. & Weaire, D. *The Pursuit of Perfect Packing* 2nd edn (Taylor and Francis, 2008).
2. Minkowski, H. Diskontinuitätsbereich für arithmetische Äquivalenz. *J. Reine Angew. Math.* **129**, 220–274 (1905).
3. Bernal, J. D. & Mason, J. Packing of spheres: co-ordination of randomly packed spheres. *Nature* **188**, 910 (1960).
4. Shannon, C. E. A mathematical theory of communication. *Bell System Tech. J.* **27**, 379–423 (1948).
5. Rogers, C. A. *Packing and Covering* (Cambridge Univ. Press, 1964).
6. Russel, W. B., Saville, D. A. & Schowalter, W. R. *Colloidal Dispersions* (Cambridge Univ. Press, 1989).
7. Prusinkiewicz, P. & Lindenmayer, A. *The Algorithmic Beauty of Plants* (Springer, 1990).
8. Conway, J. H. & Sloane, N. J. A. *Sphere Packings, Lattices and Groups* (Springer, 1998).
9. Chaikin, P. M. & Lubensky, T. C. *Principles of Condensed Matter Physics* (Cambridge Univ. Press, 1995).
10. Ellis, R. Macromolecular crowding: obvious but underappreciated. *Trends Biochem. Sci.* **26**, 597–604 (2001).
11. Cremer, T. & Cremer, C. Chromosome territories, nuclear architecture and gene regulation in mammalian cells. *Nat. Rev. Genet.* **2**, 292 (2001).
12. Torquato, S. *Random Heterogeneous Materials: Microstructure and Macroscopic Properties* (Springer, 2002).
13. Sahimi, M. *Heterogeneous Materials I: Linear Transport and Optical Properties* (Springer, 2003).
14. Graham, R. L., Lagarias, J. C., Mallows, C. L., Wilks, A. R. & Yan, C. H. Apollonian circle packings: number theory. *J. Number Theory* **100**, 1–45 (2003).
15. Aste, T., Saadatfar, M. & Senden, T. Local and global relations between the number of contacts and density in monodisperse sphere packs. *J. Stat. Mech. Theory Exp.* **2006**, P07010 (2006).
16. Parisi, G. & Zamponi, F. Mean field theory of hard sphere glasses and jamming. *Rev. Mod. Phys.* **82**, 789–845 (2010).
17. Torquato, S. & Stillinger, F. H. Jammed hard-particle packings: from Kepler to Bernal and beyond. *Rev. Mod. Phys.* **82**, 2633 (2010).
18. Hansen, J. P. & McDonald, I. R. *Theory of Simple Liquids* 4th edn (Academic, 2013).
19. Jiao, Y. et al. Avian photoreceptor patterns represent a disordered hyperuniform solution to a multiscale packing problem. *Phys. Rev. E* **89**, 022721 (2014).
20. Torquato, S. Perspective: basic understanding of condensed phases of matter via packing models. *J. Chem. Phys.* **149**, 020901 (2018).
21. Hartman, T., Mazáč, D. & Rastelli, L. Sphere packing and quantum gravity. *J. High Energy Phys.* **2019**, 48 (2019).
22. Dutta, S., Djabrayan, N. J.-V., Torquato, S., Shvartsman, S. Y. & Krajnc, M. Self-similar dynamics of nuclear packing in the early *Drosophila* embryo. *Biophys. J.* **117**, 743–750 (2019).
23. Afkhami-Jeddi, N., Cohn, H., Hartman, T., de Laat, D. & Tajdini, A. High-dimensional sphere packing and the modular bootstrap. *J. High Energy Phys.* **2020**, 1–45 (2020).
24. Royall, C. P. et al. Colloidal hard spheres: triumphs, challenges, and mysteries. *Rev. Mod. Phys.* **96**, 045003 (2024).
25. Charbonneau, P., Kurchan, J., Parisi, G., Urbani, P. & Zamponi, F. Glass and jamming transitions: from exact results to finite-dimensional descriptions. *Annu. Rev. Condens. Matter Phys.* **8**, 265–288 (2017).
26. Baule, A., Morone, F., Herrmann, H. J. & Makse, H. A. Edwards statistical mechanics for jammed granular matter. *Rev. Mod. Phys.* **90**, 015006 (2018).
27. Zaccone, A. Complete mathematical theory of the jamming transition: a perspective. *J. Appl. Phys.* **137**, 050901 (2025).
28. Alder, B. J. & Wainwright, T. E. Phase transition for a hard sphere system. *J. Chem. Phys.* **27**, 1208–1209 (1957).
29. Reiss, H., Frisch, H. L. & Lebowitz, J. L. Statistical mechanics of rigid spheres. *J. Chem. Phys.* **31**, 369–380 (1959).
30. Salsburg, Z. W. & Wood, W. W. Equation of state of classical hard spheres at high density. *J. Chem. Phys.* **37**, 798–1025 (1962).
31. Boltzmann, L. *Lectures on Gas Theory* (Univ. California Press, 1898).
32. Hoover, W. G. & Ree, F. H. Melting transition and communal entropy for hard spheres. *J. Chem. Phys.* **49**, 3609–3618 (1968).
33. Frenkel, D. Entropy-driven phase transitions. *Physica A* **263**, 26–38 (1999).

34. Mau, S. C. & Huse, D. A. Stacking entropy of hard-sphere crystals. *Phys. Rev. E* **59**, 4396–4401 (1999).
35. Bernard, E. P. & Krauth, W. Two-step melting in two dimensions: first-order liquid-hexatic transition. *Phys. Rev. Lett.* **107**, 155704 (2011).
36. Wang, H., Huse, D. A. & Torquato, S. Hole statistics of equilibrium 2D and 3D hard-sphere crystals. *J. Chem. Phys.* **161**, 074106 (2024).
37. Rintoul, M. D. & Torquato, S. Metastability and crystallization in hard-sphere systems. *Phys. Rev. Lett.* **77**, 4198–4201 (1996).
38. Kauzmann, W. The nature of the glassy state and the behavior of liquids at low temperatures. *Chem. Rev.* **43**, 219–256 (1948).
39. Woodcock, L. V. & Angell, C. A. Diffusivity of the hard-sphere model in the region of fluid metastability. *Phys. Rev. Lett.* **47**, 1129–1132 (1981).
40. Speedy, R. J. The hard sphere glass transition. *Mol. Phys.* **95**, 169–178 (1998).
41. Berthier, L., Ozawa, M. & Scalliet, C. Configurational entropy of glass-forming liquids. *J. Chem. Phys.* **150**, 160902 (2019).
42. Parisi, G. & Zamponi, F. The ideal glass transition of hard spheres. *J. Chem. Phys.* **123**, 144501 (2005).
43. Rintoul, M. D. & Torquato, S. Computer simulations of dense hard-sphere systems. *J. Chem. Phys.* **105**, 9258–9265 (1996).
44. Zhu, J. et al. Crystallization of hard-sphere colloids in microgravity. *Nature* **387**, 883–885 (1997).
45. Santen, L. & Krauth, W. Absence of thermodynamic phase transition in a model glass former. *Nature* **405**, 550–551 (2000).
46. Sciortino, F. & Tartaglia, P. Glassy colloidal systems. *Adv. Phys.* **54**, 471–524 (2005).
47. Donev, A., Stillinger, F. H. & Torquato, S. Do binary hard disks exhibit an ideal glass transition? *Phys. Rev. Lett.* **96**, 225502 (2006).
48. Pusey, P. N. et al. Hard spheres: crystallization and glass formation. *Philos. Trans. A Math. Phys. Eng. Sci.* **367**, 4993–5011 (2009).
49. Baranau, V. & Tallarek, U. Relaxation times, jamming densities, and ideal glass transition densities for hard spheres in a wide range of polydispersities. *AIP Adv.* **10**, 035212 (2020).
50. Jadrich, R. & Schweizer, K. S. Equilibrium theory of the hard sphere fluid and glasses in the metastable regime up to jamming. I. Thermodynamics. *J. Chem. Phys.* **139**, 054501 (2013).
51. Torquato, S., Truskett, T. M. & Debenedetti, P. G. Is random close packing of spheres well defined? *Phys. Rev. Lett.* **84**, 2064–2067 (2000).
52. Torquato, S. Nearest-neighbor statistics for packings of hard spheres and disks. *Phys. Rev. E* **51**, 3170–3182 (1995).
53. Reńyi, A. On a one-dimensional problem concerning random space filling. *Sel. Transl. Math. Stat. Probab.* **4**, 203–218 (1963).
54. Widom, B. Random sequential addition of hard spheres to a volume. *J. Chem. Phys.* **44**, 3888–3894 (1966).
55. Finegold, L. & Donnell, J. T. Maximum density of random placing of membrane-particles. *Nature* **278**, 443–445 (1979).
56. Feder, J. Random sequential adsorption. *J. Theor. Biol.* **87**, 237–254 (1980).
57. Swendsen, R. H. Dynamics of random sequential adsorption. *Phys. Rev. A* **24**, 504–508 (1981).
58. Cooper, D. W. Random-sequential-packing simulations in three dimensions for spheres. *Phys. Rev. A* **38**, 522–524 (1988).
59. Talbot, J., Schaaf, P. & Tarjus, G. Random sequential addition of hard spheres. *Mol. Phys.* **72**, L397–L406 (1991).
60. Torquato, S., Uche, O. U. & Stillinger, F. H. Random sequential addition of hard spheres in high Euclidean dimensions. *Phys. Rev. E* **74**, 061308 (2006).
61. Zhang, G. & Torquato, S. Precise algorithm to generate random sequential addition of hard hyperspheres at saturation. *Phys. Rev. E* **88**, 053312 (2013).
62. Tanemura, M. & Hasegawa, M. Geometrical models for territory. I. Models for synchronous and asynchronous settlement of territories. *J. Theor. Biol.* **82**, 477–496 (1980).
63. Flory, P. J. Intramolecular reaction between neighboring substituents of vinyl polymers. *J. Am. Chem. Soc.* **61**, 1518–1521 (1939).
64. Roman, E. & Majlis, N. Computer simulation model of the structure of ion implanted impurities in semiconductors. *Solid State Commun.* **47**, 259–261 (1983).
65. Torquato, S. & Stillinger, F. H. Local density fluctuations, hyperuniform systems, and order metrics. *Phys. Rev. E* **68**, 041113 (2003).
66. Torquato, S. Hyperuniform states of matter. *Phys. Rep.* **745**, 1–95 (2018).
67. Bonnier, B., Boyer, D. & Viot, P. Pair correlation function in random sequential adsorption processes. *J. Phys. A Math. Gen.* **27**, 3671–3682 (1994).
68. Torquato, S. & Stillinger, F. H. Exactly solvable disordered sphere-packing model in arbitrary-dimensional Euclidean spaces. *Phys. Rev. E* **73**, 031106 (2006).
69. Torquato, S. & Jiao, Y. Robust algorithm to generate a diverse class of dense disordered and ordered sphere packings via linear programming. *Phys. Rev. E* **82**, 061302 (2010).
70. Bernal, J. D. Geometry and the structure of monatomic liquids. *Nature* **185**, 68–70 (1960).
71. Bernal, J. D. in *Liquids: Structure, Properties, Solid Interactions* (ed. Hughel, T. J.) 25–50 (Elsevier, 1965).
72. Scott, G. D. & Kilgour, D. M. The density of random close packing of spheres. *J. Phys. D Appl. Phys.* **2**, 863–866 (1969).
73. Our Molecular Physics Correspondent What is random packing? *Nature* **239**, 488–489 (1972).
74. Gotoh, K. & Finney, J. L. Statistical geometrical approach to random packing density of equal spheres. *Nature* **252**, 202–205 (1974).
75. Berryman, J. G. Random close packing of hard spheres and disks. *Phys. Rev. A* **27**, 1053–1061 (1983).
76. Jodrey, W. S. & Tory, E. M. Computer simulation of close random packing of equal spheres. *Phys. Rev. A* **32**, 2347–2351 (1985).
77. Zinchenko, A. Z. Algorithm for random close packing of spheres with periodic boundary conditions. *J. Comput. Phys.* **114**, 298–307 (1994).
78. Jullien, R., Sadoc, J.-F. & Mosseri, R. Packing at random in curved space and frustration: a numerical study. *J. Phys. I* **7**, 1677–1692 (1997).
79. Pouliquen, O., Nicolas, M. & Weidman, P. D. Crystallization of non-Brownian spheres under horizontal shaking. *Phys. Rev. Lett.* **79**, 3640–3643 (1997).
80. Edwards, S. F. in *Granular Matter* (ed. Mehta, A.) 121–140 (Springer, 1994).
81. Liu, A. J. & Nagel, S. R. Jamming is not just cool anymore. *Nature* **396**, 21–22 (1998).
82. Edwards, S. F. & Grinev, D. V. The tensorial formulation of volume function for packings of particles. *Chem. Eng. Sci.* **56**, 5451–5455 (2001).
83. Makse, H. A. & Kurchan, J. Testing the thermodynamic approach to granular matter with a numerical model of a decisive experiment. *Nature* **415**, 614–617 (2002).
84. Silbert, L. E., Ertas, D., Grest, G. S., Halsey, T. C. & Levine, D. Geometry of frictionless and frictional sphere packings. *Phys. Rev. E* **65**, 031304 (2002).
85. O'Hern, C. S., Silbert, L. E., Liu, A. J. & Nagel, S. R. Jamming at zero temperature and zero applied stress: the epitome of disorder. *Phys. Rev. E* **68**, 011306 (2003).
86. Silbert, L. E., Liu, A. J. & Nagel, S. R. Vibrations and diverging length scales near the unjamming transition. *Phys. Rev. Lett.* **95**, 098301 (2005).
87. Wyart, M., Silbert, L. E., Nagel, S. R. & Witten, T. A. Effects of compression on the vibrational modes of marginally jammed solids. *Phys. Rev. E* **72**, 051306 (2005).
88. Gao, G.-J., Blawzdziewicz, J. & O'Hern, C. S. Understanding the frequency distribution of mechanically stable disk packings. *Phys. Rev. E* **74**, 061304 (2006).
89. Song, C., Wang, P. & Makse, H. A. A phase diagram for jammed matter. *Nature* **453**, 629–632 (2008).
90. Jin, Y., Charbonneau, P., Meyer, S., Song, C. & Zamponi, F. Application of Edwards' statistical mechanics to high-dimensional jammed sphere packings. *Phys. Rev. E* **82**, 051126 (2010).
91. Conley, G. M., Aebischer, P., Nöjd, S., Schurtenberger, P. & Scheffold, F. Jamming and overpacking fuzzy microgels: deformation, interpenetration, and compression. *Sci. Adv.* **3**, e1700969 (2017).
92. Pan, D., Wang, Y., Yoshino, H., Zhang, J. & Jin, Y. A review on shear jamming. *Phys. Rep.* **1038**, 1–18 (2023).
93. Torquato, S. & Stillinger, F. H. Multiplicity of generation, selection, and classification procedures for jammed hard-particle packings. *J. Phys. Chem. B* **105**, 11849–11853 (2001).
94. Kansal, A. R., Torquato, S. & Stillinger, F. H. Diversity of order and densities in jammed hard-particle packings. *Phys. Rev. E* **66**, 041109 (2002).
95. Torquato, S., Donev, A. & Stillinger, F. H. Breakdown of elasticity theory for jammed hard-particle packings: conical nonlinear constitutive theory. *Int. J. Solids Struct.* **40**, 7143–7153 (2003).
96. Donev, A., Torquato, S., Stillinger, F. H. & Connelly, R. Jamming in hard sphere and disk packings. *J. Appl. Phys.* **95**, 989–999 (2004).
97. Jiao, Y., Stillinger, F. H. & Torquato, S. Nonuniversality of density and disorder of jammed sphere packings. *J. Appl. Phys.* **109**, 013508 (2011).
98. Torquato, S. & Stillinger, F. H. Toward the jamming threshold of sphere packings: tunneled crystals. *J. Appl. Phys.* **102**, 093511 (2007).
99. Connelly, R., Bezdek, K. & Bezdek, A. Finite and uniform stability of sphere packings. *Discrete Comput. Geom.* **20**, 111–130 (1998).
100. Donev, A., Torquato, S. & Stillinger, F. H. Pair correlation function characteristics of nearly jammed disordered and ordered hard-sphere packings. *Phys. Rev. E* **71**, 011105 (2005).
101. Donev, A., Torquato, S., Stillinger, F. H. & Connelly, R. A linear programming algorithm to test for jamming in hard-sphere packings. *J. Comput. Phys.* **197**, 139–166 (2004).
102. Moukarzel, C. F. Isostatic phase transition and instability in stiff granular materials. *Phys. Rev. Lett.* **81**, 1634–1637 (1998).
103. Donev, A., Connelly, R., Stillinger, F. H. & Torquato, S. Underconstrained jammed packings of nonspherical hard particles: ellipses and ellipsoids. *Phys. Rev. E* **75**, 051304 (2007).
104. Stillinger, F. H. & Salsburg, Z. W. Limiting polytope geometry for rigid rods, disks, and spheres. *J. Stat. Phys.* **1**, 179–225 (1969).
105. Torquato, S. Structural characterization of many-particle systems on approach to hyperuniform states. *Phys. Rev. E* **103**, 052126 (2021).
106. Kansal, A. R., Truskett, T. M. & Torquato, S. Nonequilibrium hard-disk packings with controlled orientational order. *J. Chem. Phys.* **113**, 4844–4851 (2000).
107. Steinhardt, P. J., Nelson, D. R. & Ronchetti, M. Bond-orientational order in liquids and glasses. *Phys. Rev. B* **28**, 784–805 (1983).
108. Kansal, A. R. & Torquato, S. Prediction of trapping rates in mixtures of partially absorbing spheres. *J. Chem. Phys.* **116**, 10589–10597 (2002).
109. Truskett, T. M., Torquato, S. & Debenedetti, P. G. Towards a quantification of disorder in materials: distinguishing equilibrium and glassy sphere packings. *Phys. Rev. E* **62**, 993–1001 (2000).
110. Torquato, S., Zhang, G. & Stillinger, F. H. Ensemble theory for stealthy hyperuniform disordered ground states. *Phys. Rev. X* **5**, 021020 (2015).

111. Zachary, C. E. & Torquato, S. Hyperuniformity in point patterns and two-phase heterogeneous media. *J. Stat. Mech. Theory Exp.* **2009**, P12015 (2009).
112. Errington, J. R., Debenedetti, P. G. & Torquato, S. Quantification of order in the Lennard-Jones system. *J. Chem. Phys.* **118**, 2256 (2003).
113. Stachurski, Z. H. Definition and properties of ideal amorphous solids. *Phys. Rev. Lett.* **90**, 155502 (2003).
114. Errington, J. R. & Debenedetti, P. G. Relationship between structural order and the anomalies of liquid water. *Nature* **409**, 318–321 (2001).
115. Errington, J. R., Debenedetti, P. G. & Torquato, S. Cooperative origin of low-density domains in liquid water. *Phys. Rev. Lett.* **89**, 215503 (2002).
116. Martelli, F., Torquato, S., Giovambattista, N. & Car, R. Large-scale structure and hyperuniformity of amorphous ices. *Phys. Rev. Lett.* **119**, 136002 (2017).
117. Martiniani, S., Chaikin, P. M. & Levine, D. Quantifying hidden order out of equilibrium. *Phys. Rev. X* **9**, 011031 (2019).
118. Maher, C. E. & Torquato, S. Local order metrics for many-particle systems across length scales. *Phys. Rev. Res.* **6**, 033262 (2024).
119. Klatt, M. A. et al. Universal hidden order in amorphous cellular geometries. *Nat. Commun.* **10**, 811 (2019).
120. Torquato, S., Zhang, G. & de Courcy-Ireland, M. Hidden multiscale order in the primes. *J. Phys. A Math. Theor.* **52**, 135002 (2019).
121. Klatt, M. A., Kim, J. & Torquato, S. Cloaking the underlying long-range order of randomly perturbed lattices. *Phys. Rev. E* **101**, 032118 (2020).
122. Morse, P. K., Steinhardt, P. J. & Torquato, S. Ordered and disordered stealthy hyperuniform point patterns across spatial dimensions. *Phys. Rev. Res.* **6**, 033260 (2024).
123. Hales, T. C. A proof of the Kepler conjecture. *Ann. Math.* **162**, 1065–1185 (2005).
124. Fejes Tóth, L. *Regular Figures* (Macmillan, 1964).
125. Lubachevsky, B. D. & Stillinger, F. H. Geometric properties of random disk packings. *J. Stat. Phys.* **60**, 561–583 (1990).
126. Donev, A., Torquato, S. & Stillinger, F. H. Neighbor list collision-driven molecular dynamics for nonspherical hard particles: I. Algorithmic details. *J. Comput. Phys.* **202**, 737–764 (2005).
127. Donev, A., Stillinger, F. H. & Torquato, S. Unexpected density fluctuations in disordered jammed hard-sphere packings. *Phys. Rev. Lett.* **95**, 090604 (2005).
128. Zallen, R. *The Physics of Amorphous Solids* (Wiley, 1983).
129. Wilken, S., Guerra, R. E., Levine, D. & Chaikin, P. M. Random close packing as a dynamical phase transition. *Phys. Rev. Lett.* **127**, 038002 (2021).
130. Rissone, P., Corwin, E. I. & Parisi, G. Long-range anomalous decay of the correlation in jammed packings. *Phys. Rev. Lett.* **127**, 038001 (2021).
131. Maher, C. E., Jiao, Y. & Torquato, S. Hyperuniformity of maximally random jammed packings of hyperspheres across spatial dimensions. *Phys. Rev. E* **108**, 064602 (2023).
132. Wang, Y., Qian, Z., Tong, H. & Tanaka, H. Hyperuniform disordered solids with crystal-like stability. *Nat. Commun.* **16**, 1398 (2025).
133. Zachary, C. E., Jiao, Y. & Torquato, S. Hyperuniform long-range correlations are a signature of disordered jammed hard-particle packings. *Phys. Rev. Lett.* **106**, 178001 (2011).
134. O'Hern, C. S., Langer, S. A., Liu, A. J. & Nagel, S. R. Random packings of frictionless particles. *Phys. Rev. Lett.* **88**, 075507 (2002).
135. Charbonneau, P., Corwin, E. I., Parisi, G. & Zamponi, F. Universal microstructure and mechanical stability of jammed packings. *Phys. Rev. Lett.* **109**, 205501 (2012).
136. Atkinson, S., Stillinger, F. H. & Torquato, S. Detailed characterization of rattlers in exactly isostatic, strictly jammed sphere packings. *Phys. Rev. E* **88**, 062208 (2013).
137. Stillinger, F. H., DiMarzio, E. A. & Kornegay, R. L. Systematic approach to explanation of the rigid-disk phase transition. *J. Chem. Phys.* **40**, 1564–1576 (1964).
138. Wyart, M. Marginal stability constrains force and pair distributions at random close packing. *Phys. Rev. Lett.* **109**, 125502 (2012).
139. Kallus, Y. & Torquato, S. Marginal stability in jammed packings: quasicontacts and weak contacts. *Phys. Rev. E* **90**, 022114 (2014).
140. Torquato, S. & Kim, J. Existence of nonequilibrium glasses in the degenerate stealthy hyperuniform ground-state manifold. *Soft Matter* **21**, 4898–4907 (2025).
141. Atkinson, S., Stillinger, F. H. & Torquato, S. Existence of isostatic, maximally random jammed monodisperse hard-disk packings. *Proc. Natl Acad. Sci. USA* **111**, 18436–18441 (2014).
142. Tian, J., Xu, Y., Jiao, Y. & Torquato, S. A geometric-structure theory for maximally random jammed packings. *Sci. Rep.* **5**, 16722 (2015).
143. Barlow, W. Probable nature of the internal symmetry of crystals. *Nature* **29**, 186–188 (1883).
144. Frisch, H. L. & Percus, J. K. High dimensionality as an organizing device for classical fluids. *Phys. Rev. E* **60**, 2942–2948 (1999).
145. Skoge, M., Donev, A., Stillinger, F. H. & Torquato, S. Packing hyperspheres in high-dimensional Euclidean spaces. *Phys. Rev. E* **74**, 041127 (2006).
146. Parisi, G. & Zamponi, F. Amorphous packings of hard spheres for large space dimension. *J. Stat. Mech. Theory Exp.* **2006**, P03017 (2006).
147. Kurchan, J., Parisi, G. & Zamponi, F. Exact theory of dense amorphous hard spheres in high dimension I. The free energy. *J. Stat. Mech. Theory Exp.* **2012**, P10012 (2012).
148. Charbonneau, P., Kurchan, J., Parisi, G., Urbani, P. & Zamponi, F. Exact theory of dense amorphous hard spheres in high dimension. III. The full replica symmetry breaking solution. *J. Stat. Mech. Theory Exp.* **2014**, P10009 (2014).
149. Charbonneau, P., Hu, Y., Kundu, J. & Morse, P. K. The dimensional evolution of structure and dynamics in hard sphere liquids. *J. Chem. Phys.* **156**, 134502 (2022).
150. Wilken, S., Guo, A. Z., Levine, D. & Chaikin, P. M. Dynamical approach to the jamming problem. *Phys. Rev. Lett.* **131**, 238202 (2023).
151. Torquato, S. & Stillinger, F. H. New conjectural lower bounds on the optimal density of sphere packings. *Exp. Math.* **15**, 307–331 (2006).
152. Zachary, C. E. & Torquato, S. High-dimensional generalizations of the kagome and diamond crystals and the decorrelation principle for periodic sphere packings. *J. Stat. Mech. Theory Exp.* **2011**, P10017 (2011).
153. Andreanov, A., Scardicchio, A. & Torquato, S. Extreme lattices: symmetries and decorrelation. *J. Stat. Mech. Theory Exp.* **2016**, 113301 (2016).
154. Luban, M. & Baram, A. Third and fourth virial coefficients of hard hyperspheres of arbitrary dimensionality. *J. Chem. Phys.* **76**, 3233–3241 (1982).
155. Finken, R., Schmidt, M. & Löwen, H. Freezing transition of hard hyperspheres. *Phys. Rev. E* **65**, 016108 (2001).
156. Clisby, N. & McCoy, B. M. Ninth and tenth order virial coefficients for hard spheres in D dimensions. *J. Stat. Phys.* **122**, 15–57 (2006).
157. van Meel, J. A., Frenkel, D. & Charbonneau, P. Geometrical frustration: a study of four-dimensional hard spheres. *Phys. Rev. E* **79**, 030201 (2009).
158. van Meel, J. A., Charbonneau, B., Fortini, A. & Charbonneau, P. Hard sphere crystallization gets rarer with increasing dimension. *Phys. Rev. E* **80**, 061110 (2009).
159. Lue, L., Bishop, M. & Whitlock, P. A. The fluid to solid phase transition of hard hyperspheres in four and five dimensions. *J. Chem. Phys.* **132**, 104509 (2010).
160. Wyler, D., Rivier, N. & Frisch, H. L. Hard-sphere fluid in infinite dimensions. *Phys. Rev. A* **36**, 2422–2431 (1987).
161. Baus, M. & Colot, J. L. Thermodynamics and structure of a fluid of hard rods, disks, spheres, or hyperspheres from rescaled virial expansions. *Phys. Rev. A* **36**, 3912–3925 (1987).
162. Rohrmann, R. D. & Santos, A. Structure of hard-hypersphere fluids in odd dimensions. *Phys. Rev. E* **76**, 051202 (2007).
163. Adda-Bedia, M., Katzav, E. & Vella, D. Solution of the Percus-Yevick equation for hard hyperspheres in even dimensions. *J. Chem. Phys.* **129**, 144506 (2008).
164. Charbonneau, P., Morse, P. K., Perkins, W. & Zamponi, F. Three simple scenarios for high-dimensional sphere packings. *Phys. Rev. E* **104**, 064612 (2021).
165. Torquato, S. Reformulation of the covering and quantizer problems as ground states of interacting particles. *Phys. Rev. E* **82**, 056109 (2010).
166. Pomeau, Y. Some asymptotic estimates in the random parking problem. *J. Phys. A Math. Gen.* **13**, L193–L196 (1980).
167. Torquato, S. & Stillinger, F. H. Controlling the short-range order and packing densities of many-particle systems. *J. Phys. Chem. B* **106**, 8354–8359 (2002).
168. Viazovska, M. The sphere packing problem in dimension 8. *Ann. Math.* **185**, 991–1015 (2017).
169. Cohn, H., Kumar, A., Miller, S. D., Radchenko, D. & Viazovska, M. The sphere packing problem in dimension 24. *Ann. Math.* **183**, 1017–1033 (2017).
170. Marcotte, É & Torquato, S. Efficient linear programming algorithm to generate the densest lattice sphere packings. *Phys. Rev. E* **87**, 063303 (2013).
171. Kallus, Y., Marcotte, E. & Torquato, S. Jammed lattice sphere packings. *Phys. Rev. E* **88**, 062151 (2013).
172. Elser, V. Packing spheres in high dimensions with moderate computational effort. *Phys. Rev. E* **108**, 034117 (2023).
173. Ajtai, M. The shortest vector problem in L_2 is NP-hard for randomized reductions. In *Proc. Thirtieth Annual ACM Symposium on Theory of Computing* (*STOC '98*) 10–19 (ACM, 1998).
174. Davenport, H. & Rogers, C. Hlawka's theorem in the geometry of numbers. *Duke Math. J.* **14**, 367–375 (1947).
175. Ball, K. A lower bound for the optimal density of lattice packings. *Int. Math. Res. Not.* **68**, 217–221 (1992).
176. Vance, S. Improved sphere packing lower bounds from Hurwitz lattices. *Adv. Math.* **227**, 2144–2156 (2011).
177. Venkatesh, A. A note on sphere packings in high dimension. *Int. Math. Res. Not.* **2013**, 1628–1642 (2013).
178. Jenssen, M., Joos, F. & Perkins, W. On the hard sphere model and sphere packings in high dimensions. *Forum Math. Sigma* **7**, e1 (2019).
179. Klartag, B. Lattice packing of spheres in high dimensions using a stochastically evolving ellipsoid. Preprint at https://doi.org/10.48550/arXiv.2504.05042 (2025).
180. Campos, M., Jenssen, M., Michelen, M. & Sahasrabudhe, J. A new lower bound for sphere packing. Preprint at https://doi.org/10.48550/arXiv.2312.10026 (2023).
181. Scardicchio, A., Stillinger, F. H. & Torquato, S. Estimates of the optimal density of sphere packings in high dimensions. *J. Math. Phys.* **49**, 043301 (2008).
182. Edwin, R. Fourier inequalities and sign uncertainty. Preprint at https://doi.org/10.48550/arXiv.2505.15994 (2025).
183. Cohn, H. & Elkies, N. New upper bounds on sphere packings I. *Ann. Math.* **157**, 689–714 (2003).
184. Ruelle, D. *Statistical Mechanics: Rigorous Results* (World Scientific, 1999).
185. Cohn, H., de Laat, D. & Salmon, A. Three-point bounds for sphere packing. Preprint at https://doi.org/10.48550/arXiv.2206.15373 (2022).
186. Blichfeldt, H. The minimum value of quadratic forms and the closest packing of spheres. *Math. Ann.* **101**, 605–608 (1929).
187. Kabatiansky, G. A. & Levenshtein, V. I. On bounds for packings on a sphere and in space. *Probl. Inf. Transm.* **14**, 1–17 (1978).

188. Cohn, H. & Zhao, Y. Sphere packing bounds via spherical codes. *Duke Math. J.* **163**, 1965–2002 (2014).
189. Sardari, N. T. & Zargar, M. New upper bounds for spherical codes and packings. *Math. Ann.* **389**, 3653–3703 (2024).
190. Gardner, M. *The Colossal Book of Mathematics: Classic Puzzles, Paradoxes, and Problems* (Norton, 2001).

Acknowledgements
The author is grateful to the US National Science Foundation for the support of this work over the past two decades. He thanks C. Maher, Y. Jiao, J. Kim, M. Skolnick and C. Vanoni for the helpful feedback.

Competing interests
The author declares no competing interests.

Additional information
Peer review information *Nature Reviews Physics* thanks Adrian Baule, Shuixiang Li and Vasili Baranau for their contribution to the peer review of this work.

Publisher's note Springer Nature remains neutral with regard to jurisdictional claims in published maps and institutional affiliations.

Springer Nature or its licensor (e.g. a society or other partner) holds exclusive rights to this article under a publishing agreement with the author(s) or other rightsholder(s); author self-archiving of the accepted manuscript version of this article is solely governed by the terms of such publishing agreement and applicable law.

© Springer Nature Limited 2026